Renewable and Sustainable Energy Reviews 16 (2012) 2494–2515

Contents lists available at SciVerse ScienceDirect

Renewable and Sustainable Energy Reviews

journal homepage: www.elsevier.com/locate/rser

Materials, morphologies and structures of MEAs in DMFCs

S.K. Kamarudin[a,b,*], N. Hashim[a]

[a] Fuel Cell Institute, Universiti Kebangsaan Malaysia, 43600 UKM Bangi, Selangor, Malaysia
[b] Department of Chemical and Process Engineering, Universiti Kebangsaan Malaysia, 43600 UKM Bangi, Selangor, Malaysia

ARTICLE INFO

Article history:
Received 13 June 2011
Accepted 29 January 2012
Available online 20 March 2012

Keywords:
Direct methanol fuel cell
Membrane electrode assembly
Mass transport

ABSTRACT

Even though direct methanol fuel cells (DMFCs) were developed to support power needs, there are still unresolved drawbacks. The main focus of this research is the membrane electrode assembly (MEA), which is the most important component of the fuel cell. The MEA consists of a combination of the diffusion layer, the electrode layer and a membrane. Several obstacles may interfere with the functioning of the MEA, including its relatively low anode electro-catalytic activity, methanol crossover and mass transport. In this paper, an overview of the layer and engineering challenges associated with the MEA will be presented in detail. This paper will also discuss the materials while focusing on the current problems, structure layers, morphologies and fabrication methods of MEAs in DMFCs.

Contents

1. Introduction

Direct methanol fuel cells (DMFCs) provide significant advantages such as high energy density, low pollution, few safety concerns, rapid start-up, low weight, simplicity, small size compared to rechargeable batteries and ease of recharging for portable applications [1–3]. Basically, there are two orientations of fuel cells that are constantly being optimized by researchers: passive- (air-breathing) and active-oriented fuel cells. However, the major problems with DMFCs result from the MEA, which is the heart of the fuel cell, and not from the orientation of the system. The MEA is composed of an electrolyte membrane located between an anode electrode and a cathode electrode. The anode and cathode electrodes consist of a catalyst layer (CL) and a gas diffusion layer (GDL). Fig. 1 shows the basic modern MEA layer in DMFCs. Normally, methanol diffuses from the reservoir through the GDL and into the CL, where it is oxidized to carbon dioxide. In the cathode, oxygen from the surrounding air is transferred through the GDL and into the CL, where it is reduced to water. At the same time, free electrons from the anode reactions flow through the external circuit to the cathode, which allows the reaction at the cathode to continue. Before the electrons reach the external circuit (current collector), they must be able to flow through the CL and GDL. To ensure that these reactions continue smoothly, the materials, structures and layers must support and react accordingly. By optimizing every layer in the MEA, several barriers can be removed, such as methanol crossover, electro-catalytic activity, transport and management issues (fuel, removal, heat, water, gas, etc.), conduction

* Corresponding author. Tel.: +60 3 89216422; fax: +60 3 89216148.
E-mail addresses: ctie@vlsi.eng.ukm.my, ctie@eng.ukm.my (S.K. Kamarudin).

1364-0321/$ – see front matter © 2012 Elsevier Ltd. All rights reserved.
doi:10.1016/j.rser.2012.01.073

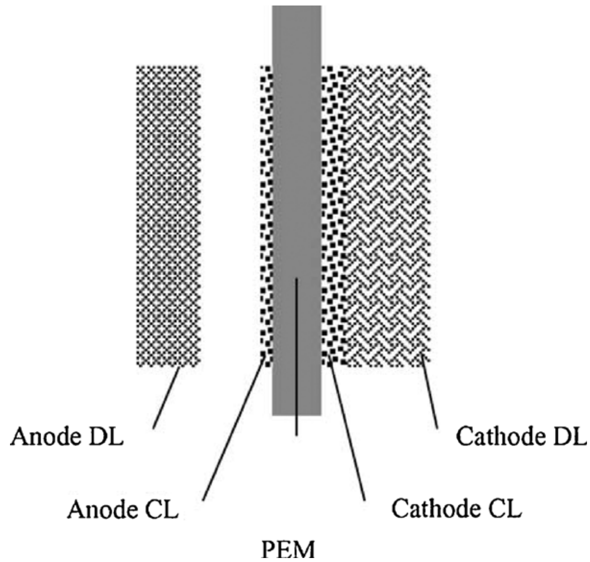


Fig. 1. Schematic of MEA in DMFC [4].

and distribution can be enhanced. Conventional MEA for DMFCs consist of a GDL, a CL and a membrane.

2. Functions and challenges in MEA layers

2.1. Gas diffusion layer (GDL)

In DMFCs, the first layer in contact with the fuel (methanol and oxygen) is the gas diffusion layer (GDL). The GDL typically consists of a backing layer containing a macroporous substrate and a microporous layer (MPL) made from carbon powder. The GDL is required to maintain water balance in the membrane electrode assembly (MEA) by allowing the appropriate amount of water to move in and out of the reaction zone, to provide mechanical support for the MEA and to provide electrical contact between the electrodes and the current collectors during operation of the fuel cell. The GDL can be divided into an anode gas diffusion layer (AGDL) and a cathode gas diffusion layer (CGDL). Both sides must handle different reactants and removal products. The major issues with the GDL can be classified into three categories: (1) reactant distribution, (2) water and gas management and (3) electrical contact and conductivity [5]. Therefore, the GDL plays an important role in providing preliminary support for the entire MEA operation.

In DMFCs, liquid methanol normally must be transported through the AGDL via diffusion to the catalyst layer for the reaction to occur. A uniform distribution of fuel is required to ensure that the appropriate amount of methanol is distributed over the entire area of the catalyst layer. Once the reaction begins, CO_2 formed as a byproduct must be removed. Therefore, both liquid and gas phase transport paths must be provided to reduce the polarization effect due to anode mass transport in the DMFCs [4]. So far, no ideal solutions have been developed for managing mass transport for the gas and liquid phases at the anode and cathode sides.

Möst et al. [6] reported that the effective transport coefficient of the porous GDL has a major influence on limiting the current density. They also indicated that the correlation between porosity and tortuosity strongly influences the mass transport coefficient. The tortuosity increased as the porosity decreased, which caused the effective transport coefficient to decrease due to the high mass transfer resistance. Park and Popov [7] mentioned that another important consideration for improving the performance of the GDL in terms of mass transfer relies on the microporous layer (MPL). An MPL with a high volume of micropores and increased hydrophobicity was able to provide effective water removal and gas permeability.

The designs of the anode and cathode GDLs are similar, but the cathode diffusion layer allows gases to move through the catalyst layer and is capable of removing water, while the anode GDL allows diluted methanol to move through it and remove carbon dioxide. Typically, carbon-based materials such as carbon paper or carbon cloth have been used as GDLs. Carbon is a hydrophilic material, and it has been suggested that some characteristic tuning must be performed to change its wetting characteristics to effectively prevent water accumulation and improve the limitation of transport [5].

Previous researchers such as Huang et al. [5], Xu et al. [8], and Krishnamurthy and Deepalochani [9] have suggested adding polytetrafluoroethylene (PTFE) or fluorinated ethylene propylene (FEP) to the GDL to improve anode and cathode mass transfer. However, there has been some disagreement regarding the use of a hydrophobic material to solve this problem because hydrophobic materials may decrease the pore size and decrease the mass transfer coefficient due to the increased flow resistance. For example, Xu et al. [4] reported that treating the diffusion layer with PTFE decreased the limiting current density due to the increased mass transfer resistance and suggested that the GDL does not need to be treated with PTFE. However, Krishnamurthy and Deepalochani [9] found that PTFE played an important role in the performance of DMFCs. When the appropriate amount of hydrophobic material was added to the GDL, the performance of the DMFC was improved. Mass transfer resistance became ideal with the presence of this material. Further experimental work, material–structure analysis and fast screening activity could help increase the performance of DMFCs. Recent developments using nanotechnology approaches to address the mass transfer issues with the GDL may create more stable and reliable GDL materials and structures for application in DMFCs.

2.2. Catalyst layer (CL)

The main function of the catalyst layer in the DMFC system is to accelerate the reaction activity to obtain the highest kinetic reactivity rate for methanol oxidation and oxygen reduction at the anode and cathode, respectively. Furthermore, the CL also plays important roles such as conducting protons and electrons, supplying reactants (oxygen and methanol) and removing products (heat, water and carbon dioxide); in simple terms, the CL should have a triple-phase boundary [10]. Several studies investigating the mechanism of the CL have been conducted by many researchers. However, the CL is still hampered by the kinetic limitations and the functioning of both the anode and cathode. In addition to its kinetic problems, methanol crossover, layer resistance and mass transport also decrease the performance of the CL. Fig. 2 shows the relationships among these issues and their effects on the CL. To solve these problems, a large amount of effort has been directed toward improving catalyst activity, catalyst layer structure and morphology, material modification and other parameters [12].

The major losses in performance at the anode were associated with poor electrochemical activity toward the methanol oxidation reaction (MOR). The reactions at the anode are very complex and create many chemical intermediates. To overcome this problem, it is necessary to understand the detailed mechanism of the MOR; methanol is oxidized by the catalyst via dehydrogenation and chemisorption, and CO is generated as an intermediate [13]. The use of platinum in DMFCs results in several challenges with chemical intermediates. The intermediates adsorb to the active sites of the Pt catalyst, thus slowing the electro-oxidation kinetics [14,15] and resulting in major impairments of catalytic activity at the anode. To effectively oxidize CO to CO_2 from methanol oxidation, high overvoltage conditions are necessary, which leads to decreased

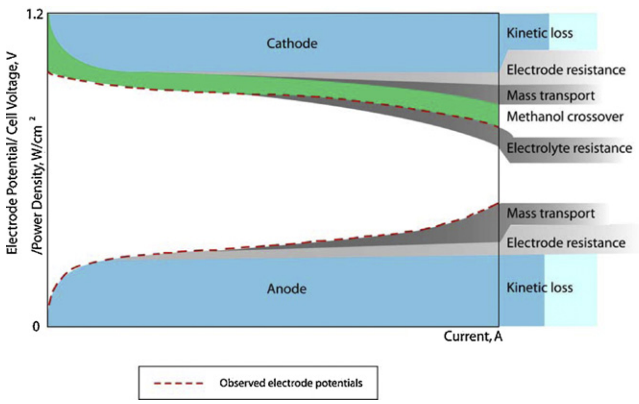


Fig. 2. Performance losses related to catalyst layer obstacles [11].

electrical performance in DMFCs [15]. While at the cathode, the reduction of oxygen on the platinum catalyst in the presence of electrons and protons generates water. Generally, the highly irreversible oxygen reduction reactions (ORRs) allowed the cathode to face the high over-potential, and about 0.2 V were lost [16,17]. The need for more active and less expensive ORR catalysts to improve ORR activity and stability over Pt-based catalysts has led to the development of binary and ternary Pt alloys [17,18]. To produce better CLs, knowledge about electrocatalyst limitations is important. Further details on the catalyst material as a solution to this problem will be explained in Section 3.

The mass transport effect also seems to be a performance-limiting factor for the anode and cathode CLs. At the anode, the CO_2 bubble generated from methanol oxidation may also block the catalyst surface and may prevent further oxidation of methanol. While at the cathode, water generated from oxygen reduction becomes a major problem because of the flooding problem it creates by blocking the pore structures and limiting the movement of air into the layer, which increases the mass transfer resistance. Furthermore, the diffusion of water and methanol from the anode to the cathode leads to another problem. Methanol that crossed through the polymeric membrane can create a mixing potential at the cathode side, which lowers the overall performance. Among all of the polymer electrolyte fuel cells (PEFCs), even under open circuit conditions, DMFCs are the most prone to problems due to methanol crossing over from the anode to the cathode, which results in a severe potential loss of approximately 0.1 V [17]. Basically, over-potential was caused by slower kinetics due to the catalyst material, even when pure Pt was used. Therefore, the mass transport issues in the CL should not be neglected. An effective catalyst layer must be constructed on both sides to improve mass transfer. Generally, mass transport was influenced by the structure and behavior of the CL. This problem can be solved by modifying the structure and thus improving the layer behavior.

Another problem contributing to performance deterioration is layer resistance. It is interesting to note that the layer structure and surface morphology affect the layer resistance and interfacial properties. The surface of the layer must be smooth with few cracks for ideal performance. According to Wang et al. [10], low resistance at the interface helps fuel, protons, electrons and products transfer effectively between the layers. The most critical location that needs to be addressed is the contact point between the CL and the membrane. The catalyst in the CL needs to directly contact the membrane to ensure sufficient proton transfer after the reaction occurs. This results in decreased resistance when the catalyst is in ionic contact with the membrane. On the other hand, resistance between the GDL and CL must be minimized because electronic conductivity depends on it. Electrons are taken away from the CL at the anode and supplied to the CL at the cathode to help the reaction continue smoothly and ensure sufficient electrical contact between the CL and GDL. The layer-preparing method seems to be one of the active effecting parameters in improving the structures of the layers. Furthermore, the selection of materials with ionic and electronic conductivity for the CL also contributes to reduction of the layer resistance.

2.3. Membrane

The MEA is not complete without a membrane to act as an electronic insulator between the anode and cathode electrodes. The MEA allows protons to travel through its sulfonic groups from the anode to the cathode. This is the main function of the membrane in DMFCs. Furthermore, the membrane also works as a physical barrier to avoid mixing of the reactants. The membrane of the DMFC should ideally exhibit the properties of an electrolyte (high proton conductivity) and a barrier (low permeability toward DMFC species). The membrane should also exhibit high chemical, mechanical and thermal stability to withstand abrasive conditions, including temperature effects, catalyst reactions, reactive radicals and strong oxidants [19–22].

Nafion membranes are normally used in DMFCs. A common problem related to this type of membrane is the diffusion of methanol through the membrane, which results in an effect known as methanol crossover [21]. This problem becomes a major obstacle in the membrane architecture of fuel cells. Methanol crossover may result from methanol diffusion and electro-osmotic drag through the membrane from the anode side to the cathode side. It not only decreases the utilization of the fuel, but it also leads to significant decreases in cathode performance and produces extra heat to the overall system. In addition, methanol crossover also accelerates membrane degradation, which shortens the life of the MEA and the cell. Generally, there are three basic approaches to handle this problem: make sure methanol is well oxidized at the anode (more related to catalyst capability), make sure no methanol reaches the cathode (membrane modification) and make sure the methanol does not react with the cathode if it does cross the membrane (cathode modification). To date, extensive efforts have been dedicated to address this methanol crossover problem.

According to Ahmad et al. [20], membranes based on sulfonated polymers such as Nafion greatly rely on water molecules for proton conductivity. High water uptake is a basic requirement for sulfonated polymer membranes to effectively conduct protons. However, it is necessary to control water uptake because if the water surpasses the limit, the membrane will exhibit undesired side effects, such as excess swelling, mechanical fragility, low dimensional stability and high methanol permeability. Typically, with sufficient humidity, these types of membranes offer effective performance below 90 °C.

3. Materials, structures and morphologies

3.1. Gas diffusion layer (GDL)

The GDL typically has a dual-layer structure, as illustrated in Fig. 3 [23]. The first layer is a backing layer (BL), which serves as a substrate for the second layer and the catalyst layer. The second layer of the GDL is a microporous layer (MPL), which consists of carbon black powder and a hydrophobic agent. Each layer in the GDL acts as a diffusion layer for gas and liquid transport in DMFC.

Materials made of carbon fiber such as carbon paper and carbon cloth were commonly chosen by researchers as the BL material because they satisfy the necessary criteria [8]. Carbon paper and carbon cloth (Fig. 4(a) and (b)) have high porosity (more than 70%)

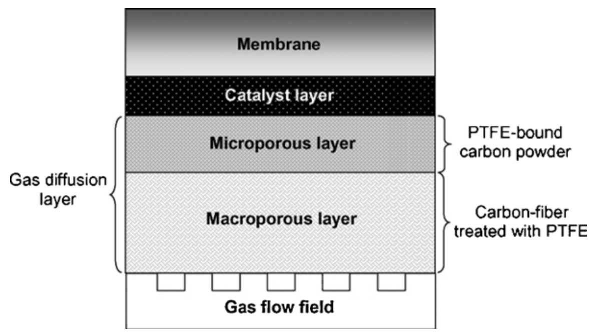


Fig. 3. Schematic diagram of a GDL [23].

and are capable of providing support to the MEA layer. The material for the BL must also be a heat and electronic conductor and a substrate for electrocatalysts [6,8,12,24–29]. However, carbon fiber-based materials have several disadvantages. The fragile structure of carbon fiber-based materials allows them to be crushed easily under high pressure, such as that of the hot press process [4]. A current collector or uneven gasket could crush it during cell assembly, which would increase the transfer resistance and deteriorate cell performance. Extra caution must be taken to choose optimum pressures during the hot press and assembly to avoid structure failure. To address the problems related to mechanical stability and strength, Liu et al. [24] and Hottinen et al. [30] proposed using a BL composed of sintered metal fibers. This material has benefits over carbon-based materials because of its structure advantages, including high mechanical strength, ductility and good electrical conductivity. Sintered metal also allows gas channels to form directly inside the metal layer during the sintering process. Metal fibers exhibit a coarser fiber surface compared to carbon paper (refer to Fig. 4(c)), which makes the material more hydrophilic and increases methanol transfer at high current densities [24].

The microporous layer (MPL) is added to the backing layer to form the gas diffusion layer (GDL). The existence of the MPL reduces water crossover, increases methanol utilization and improves cell performance [32]. The main functions of the MPL are to distribute the reactants uniformly over the electrode surface and to connect the catalyst and backing layers. Similar to the backing layer, the MPL also requires porosity to promote mass transport for the reactants, removal of the products, heat and electronic conductivity and to act as a substrate for electrocatalysts.

Carbon black is the most common material used for the MPL. Basically, carbon black is produced by heating any rich carbon-containing materials in a limited oxygen atmosphere at a high temperature [33]. Carbon black, an amorphous form of carbon, usually consists of near-spherical particles of graphite typically below 50 nm in diameter, which may join together into particle aggregates and agglomerates around 250 nm in diameter [31]. Fig. 5(a) shows an image of carbon black in high resolution. Carbon black particles under the electron microscope show a complicated structure with some spherical particles fused together. The size of the spherical particles is called the “particle size,” and the size of the particle chain is called the “structure.” Various functional groups such as hydroxyl or carboxyl groups are found on the surface of carbon black [34], and their amount or composition is called “surface chemistry.” These three properties, “particle size,” “structure,” and “surface chemistry,” are the basic properties of carbon black and are collectively known as the three main characteristics. These three characteristics have a profound effect on practical properties such as blackness and dispersibility when they are mixed with inks, paints, or resins.

Carbon nanotubes (CNTs) and carbon nanofibers (CNFs) are the most well-known forms of nanostructured carbon, and they have shown promising results as MPL materials for fuel cell applications due to their unique electrical and structural properties in enhancing the transportation in DMFCs. These carbon nano-sized materials generally exhibit better performance due to their special structure, better crystallinity, and faster mass transfer compared to other commercial materials. Fig. 5(b) and (c) shows the TEM images of these two materials. Carbon nanotubes are considered to form a curved graphene sheet. Graphene sheets are seamless cylinders derived from a honeycomb lattice and represent a single atomic layer of crystalline graphite. The ends of a nanotube may be capped with a hemisphere of the buckyball structure. Conventional carbon nanotubes are made of seamless cylinders of hexagonal carbon networks and are synthesized as single-wall (SWCNTs) or multiwall carbon nanotubes (MWCNTs). SWCNTs consist of a single graphene sheet rolled into a cylinder, and MWCNTs consist of several coaxially arranged graphene sheets rolled into a cylinder [34]. CNFs possess unique morphologies with sidewalls composed of angled graphite sheets. This morphology provides a fiber with exposed edge planes along the entire surface of the fiber and allows chemical modification of the fiber surface. The unique combination of high specific surface area, flexibility, and superior directional strength makes such fibers a preferred material for many applications from clothing to reinforcements for aerospace structures [33]. A remarkable property of CNTs and CNFs is their ability to entrap atoms of other elements within their molecular structure [35].

Wu et al. [36] revealed that the use of CNTs in the MPL may influence mass transport and consequently affect cell performance. CNTs were found to be a promising material for fabricating crack-free MPLs, which can significantly optimize mass transfer compared to carbon black, which is prone to form a large number of mud cracks with a width about 10 μm across the whole surface of the MPL. Fig. 6 shows SEM images of the MPL layer with carbon black and CNTs as source materials. It is clearly shown that the use CNTs resulted in a surface morphology free from mud-cracks. Yuan et al. [35] also mentioned this morphological characteristic.

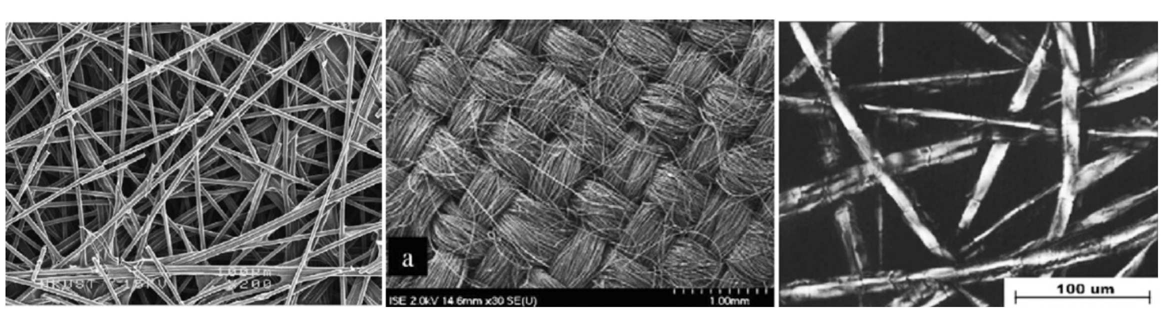


Fig. 4. SEM images of (a) carbon paper [4] (b) carbon cloth [31] and sintered stainless [24] steel structure.

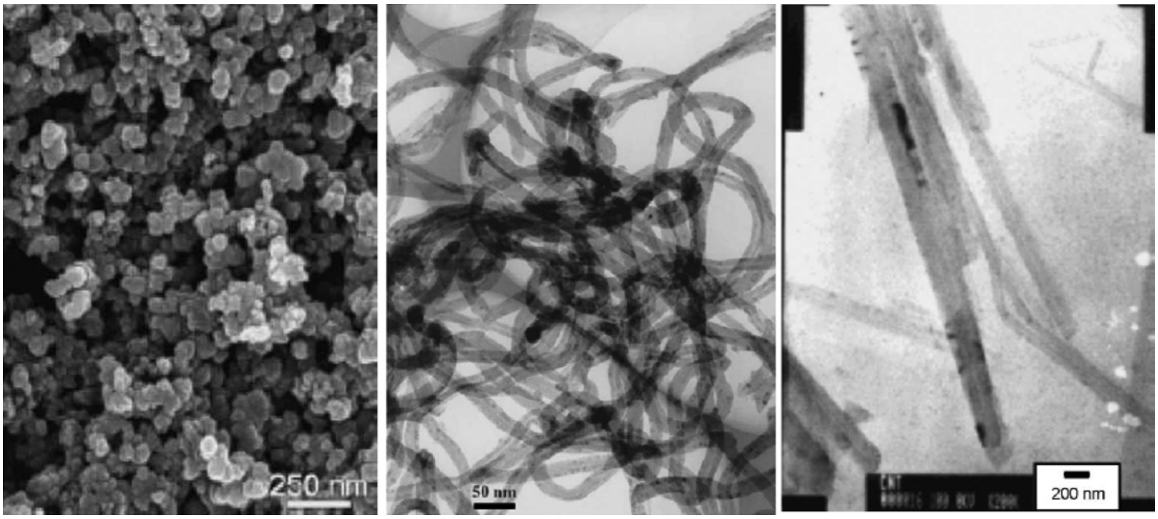


Fig. 5. TEM images of (a) carbon black, (b) CNFs and (c) CNTs [34].

For the MPL using carbon black, accumulation of a carbon ball led to poor pore distribution. The microstructure with the CNTs exhibited more uniform pore distribution and a continuous network within the layer, which was beneficial to mass transfer, catalyst utilization and electron conductivity. Fig. 7 shows SEM images of MPL morphology with carbon black and CNTs developed by the author.

CNFs as the primary components of the MPL also exhibited improved performance in terms of mass transfer, catalyst utilization and conductivity. Okada et al. [37] presented that CNFs were effective in covering and closing the large openings of the surface of the carbon paper and providing a thin and dense layer on the carbon paper. It could be seen in Fig. 8 that the nano-fibers covered the openings of the surface of the carbon paper and closed the openings, which reduced the size from several hundred to less than one hundred micrometers or smaller.

Park et al. [23] and Wang et al. [38] studied the effect of carbon loading in the microporous layer. They found that proper carbon loading was beneficial to the conduction of electrons, the diffusion of reactants, the balancing of water (water management) and lowered the mass transfer resistance. At the same time, Wu et al.

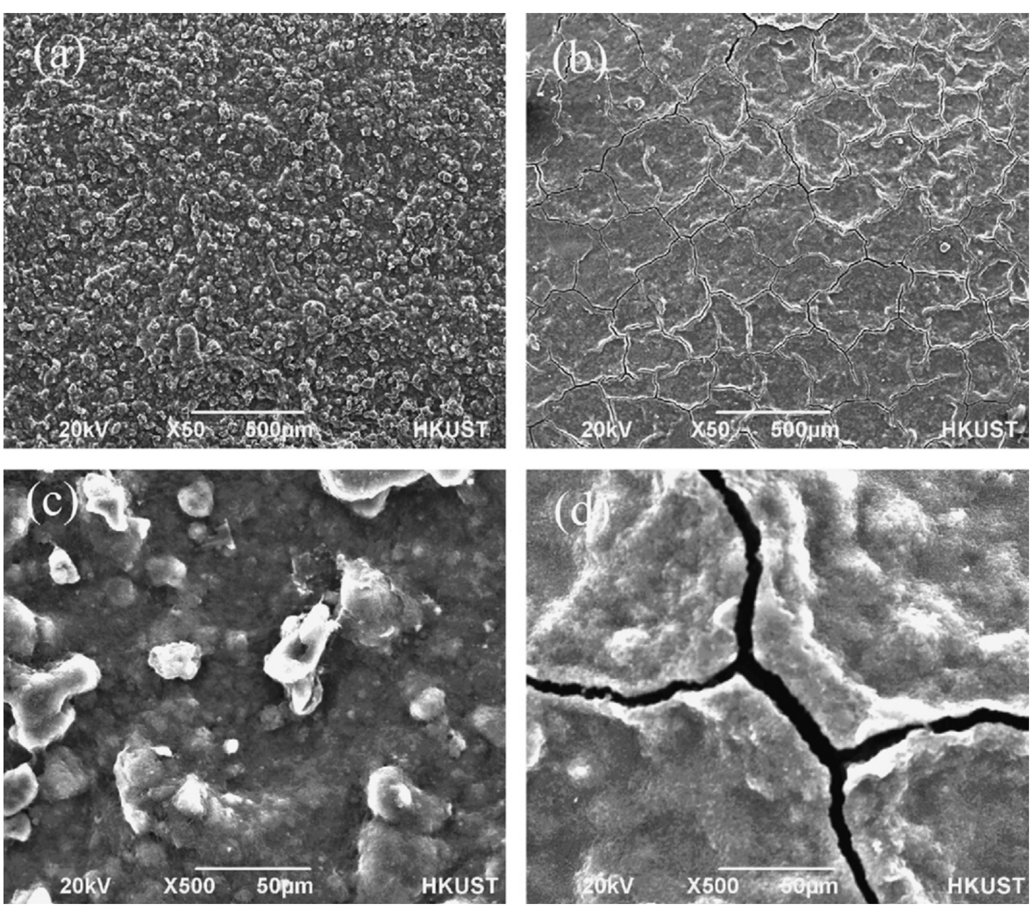


Fig. 6. Surface morphologies of various anode MPLs: (a) and (c) nanotube MPL; (b) and (d) carbon-powder MPL [36].

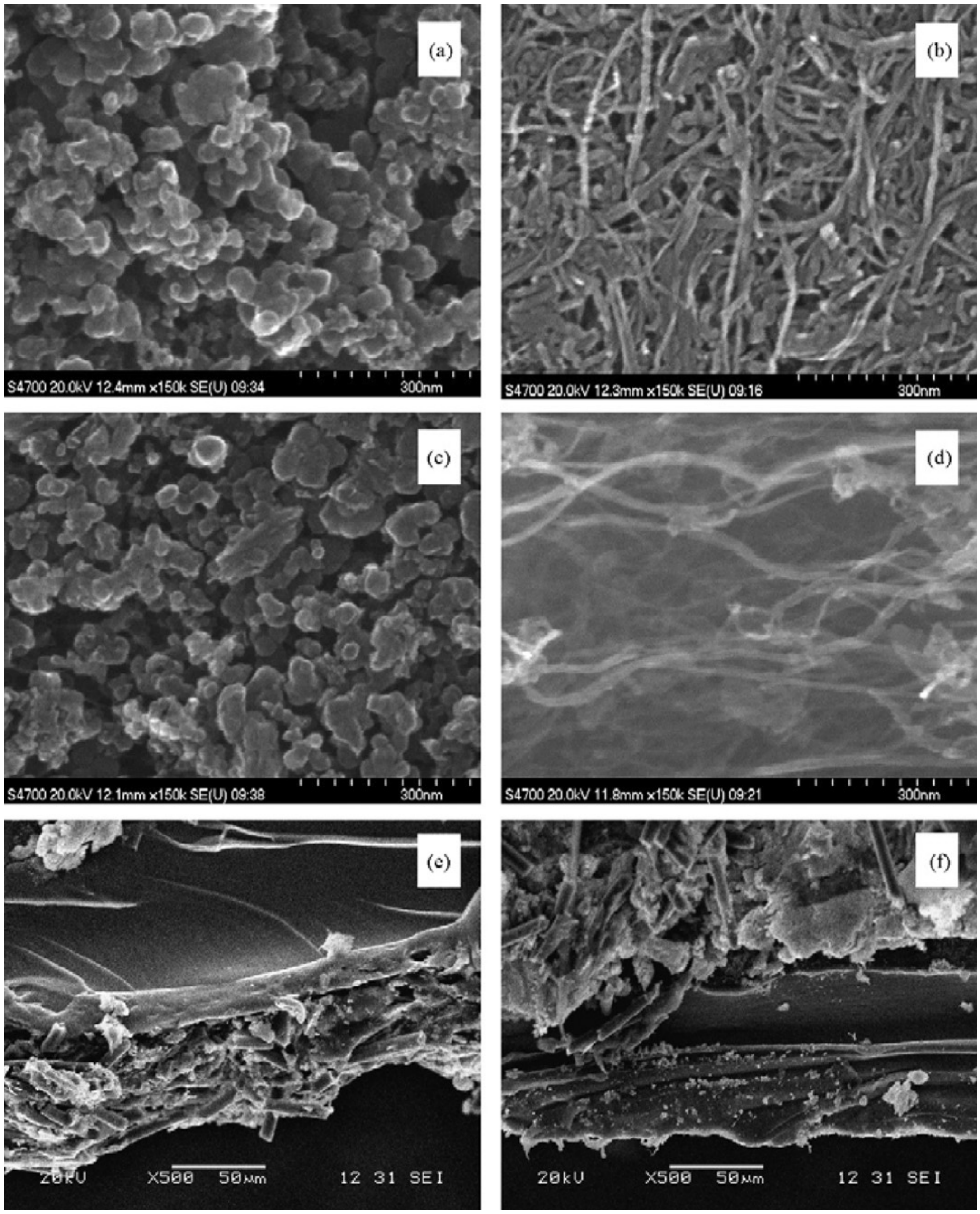


Fig. 7. Top view of SEM image of the MPL with carbon black (a) and CNTs (b); side-views of SEM images MPLs with carbon black (c) and CNTs (d); cross-sectional views of SEM images of the MEA using pure CNTs as anodic MPL materials before (e) and after (f) long-term operation [35].

[36] proved that increasing MPL loading decreased the total water crossover flux because higher carbon loading increases the thickness of the MPL, which increases the water-transfer resistance. However, this effect results in another problem similar to mud cracks, which increase the MPL permeability even when nanostructured materials are used [37]. Thus, minimizing the mud cracks is more important than increasing the MPL loading for lowering water crossover.

Studies on the use of PTFE in the BL as a hydrophobic material for water crossover flux have been performed. Although PTFE is a water repellent material, which increases the hydrophobicity of the BL [39], Xu et al. [8] found that increasing the PTFE content in the BL does not increase the performance of the cell. Fig. 9 clearly shows the performance from a previous study by Xu et al. [8] on the effect of PTFE in the BL. Layers with increased hydrophobicity rapidly removed water from the inside of the BL. However, the structure of the layer changed. The pore size and the porosity decreased with increasing PTFE content. Tseng and Lo [40] mentioned that PTFE loading changes the BL structure by decreasing the pore size, which affects the overall pore size distribution within the layer. Fig. 10 presents the pore size distribution of the carbon paper with different PTFE loading. For the 40 wt.% PTFE loading sample, nearly 70% of the pores were smaller than 4.0 μm, although the pore size ranged from 0.32 to 24.59 μm. This influences mass transport, especially at the cathode, because it lowers gas permeability. This leads to a higher mass transport resistance [9,39,41]. This was also proved by Krishnamurthy and Deepalochani [9] by analyzing the impedance response for various PTFE contents in the BL. Fig. 11 shows the impedance response analyses for various percentages of PTFE. Overall resistance can be derived from the intersection of the high frequency arc with the real axis, while the mass transfer resistance can be obtained from the low frequency curves of the

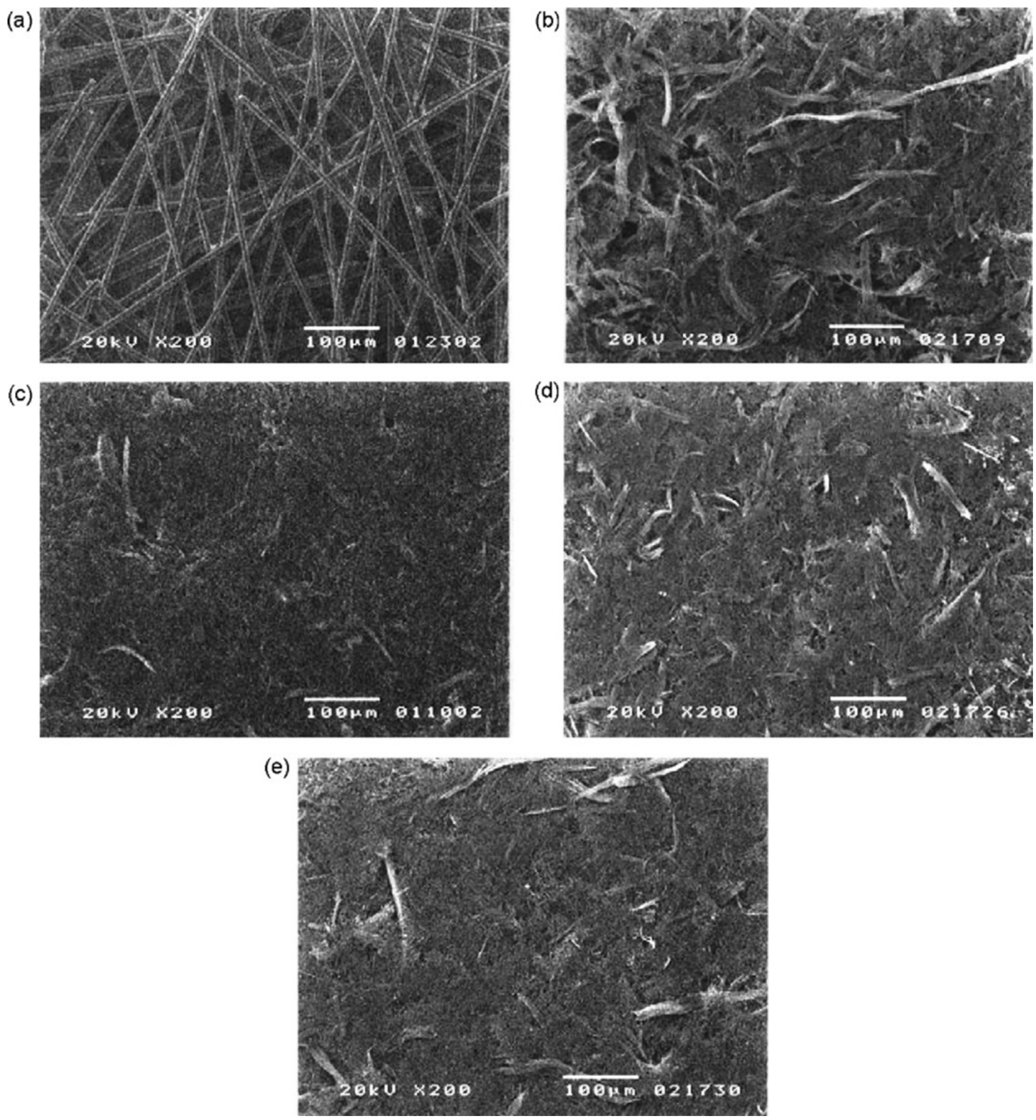


Fig. 8. SEM photographs taken of the surface of the carbon paper, (a) and that of the CNF interlayer with different amounts: (b) 0.9 mg-CNF cm^{-2}, (c) 2.1 mg-CNF cm^{-2}, (d) 2.6 mg-CNF cm^{-2}, and (e) 3.0 mg-CNF cm^{-2} [37].

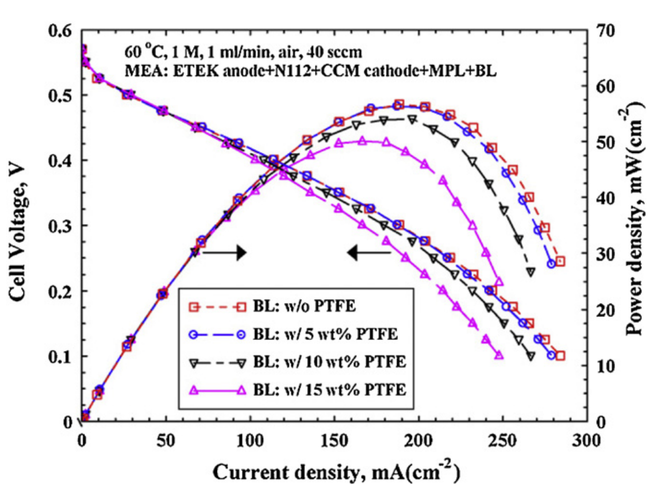


Fig. 9. Effect of the PTFE loading in the cathode BL on the cell performance [8].

impedance plot. The larger percentages of PTFE loadings in the BL led to blocked pores that restricted oxygen transport and hindered water removal, thus affecting the performance of the cell. [8,9,39].

Zhang et al. [42] stressed the importance of these two contrary behaviors gained from adding PTFE or Nafion. The performance of the cell tended to decline with increasing hydrophobic content (PTFE), especially in the anode, due to the increased difficulty of methanol transport. Increasing the PTFE content also increased the GDL contact angle and decreased the wettability. Contact angle values define the capability of liquid methanol solution to spread over or wet the surface. Higher values of the contact angle indicate poor wetting properties and increase the methanol transfer resistance throughout the GDL [36]. Another issue associated with the hydrophobic and hydrophilic properties of the MPL is the formation of CO_2 gas bubbles at the anode. Fig. 12 (taken from Zhang et al. [42]) shows an image of two MPLs with different PTFE percentages; one is more hydrophobic than the other. For the higher percentage hydrophobic anode MPL (Fig. 12(a)), the bubbles gathered at certain locations and formed larger bubbles (about 0.5–2.0 mm). For the lower percentage hydrophobic anode MPL (Fig. 12(b)), the bubbles appeared to be smaller (about 0.5–1.5 mm), and from the visualization of the CO_2 gas bubbles, it was found that these small bubbles

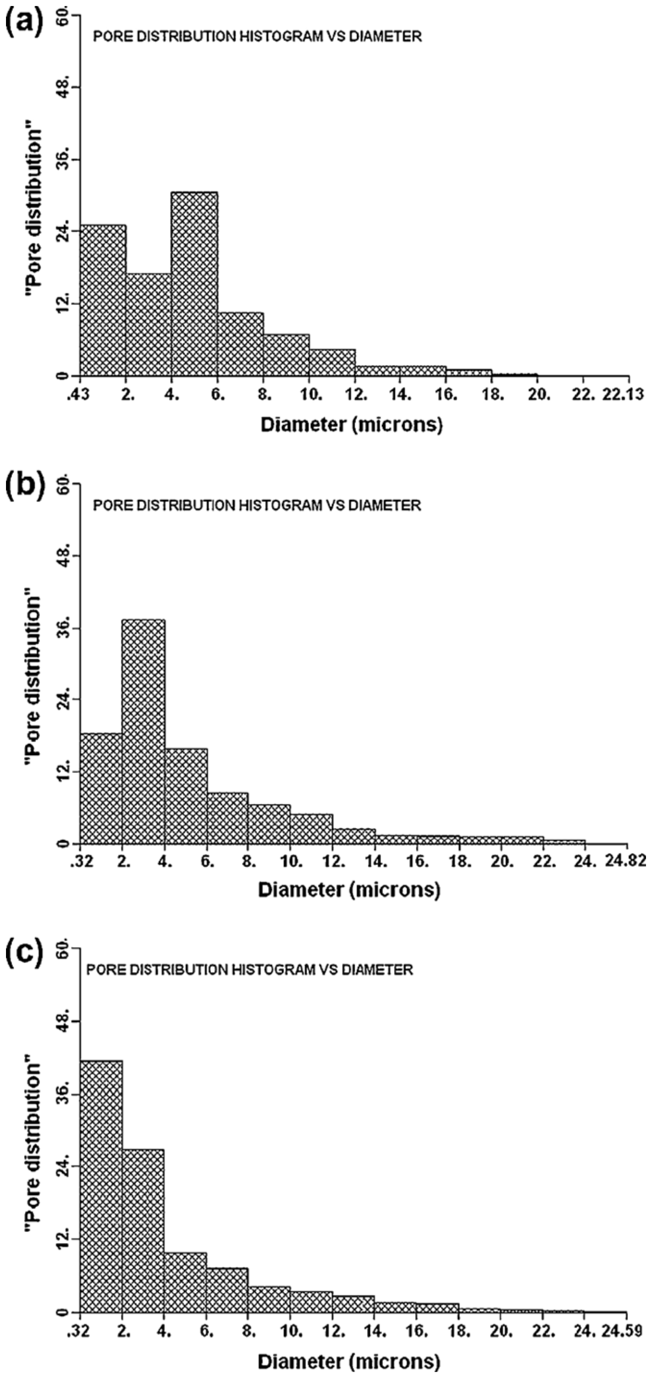


Fig. 10. Pore size distributions in carbon paper. (a) 0 wt.% PTFE loading, (b) 20 wt.% PTFE loading, and (c) 40 wt.% PTFE loading [40].

were formed uniformly. When it was easier for the bubbles to leave the anode GDL, methanol transportation resistance decreases and avoids major bubble blockage in the cell.

PTFE loading in the MPL affected the layer in several ways. By adding the hydrophobic material, Wu et al. [36] found that the PTFE content in the MPL had a small effect on the water-crossover flux because of the formation of mud cracks, which increased the permeability of the MPL and compensated for the increased hydrophobicity. On the other hand, Krishnamurthy and Deepalochani [9] found higher PTFE content results in increased mass-transfer resistance of methanol as a result of the enhanced hydrophobic level results and an inadequate methanol concentration in the anode CL, thus decreasing the cell performance.

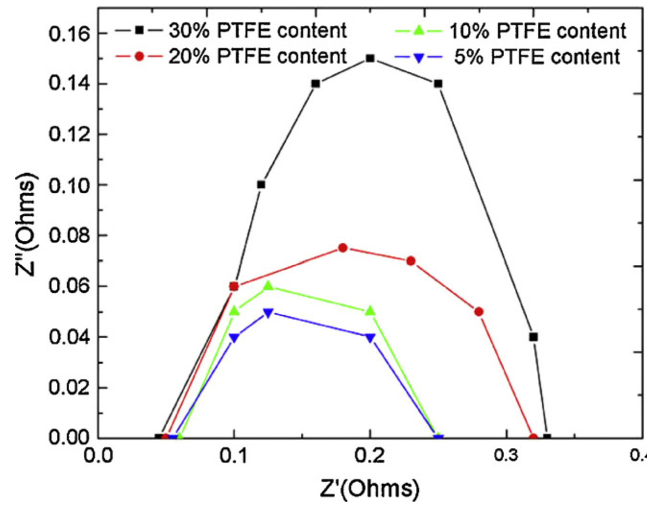


Fig. 11. Impedance response analyses for variation of PTFE content in BL [9].

However, their study came to a unique conclusion that the increased mass-transfer resistance of methanol on the anode was not actually a result of the higher PTFE loading in the MPL. They found that higher PTFE loading reduced methanol crossover so that the DMFC could be operated at a higher methanol concentration. Fig. 13 demonstrates their conclusion because the differences in performance with different PTFE loadings became much smaller when the methanol concentrations increased from 1.0 M to 2.0 M.

3.2. Catalyst layer (CL)

Platinum (Pt) is an effective and popular material used in the cathode catalyst layer, while alloyed platinum–ruthenium (Pt–Ru) is commonly used as a catalyst in the anode catalyst layer. Catalysts supported by carbon (Pt/C or Pt–Ru/C) are used to increase the surface area and to reduce the cost of the catalyst in the CL at the anode and the cathode. At the anode, Ru has to be combined with Pt to promote the oxidation of the intermediate product. It is well known that the oxidation of methanol on platinum catalysts alone generates CO as the intermediate, which adsorbs to the active sites of Pt and slows the kinetics. With the presence of the secondary metal, Ru forms oxygenated species at a lower potential than Pt and promotes further oxidation of CO to CO_2, which helps accelerate the kinetics. This interaction between Pt and Ru allows completion of the oxidation process of methanol and is called the bifunctional mechanism. Other than Ru, other metals (including Ni, Sn, Rh, Os, Re, Mo, and W, denoted by M) [43–47] have been investigated by researchers to improve the CO tolerance based on the bifunctional mechanism and the electronic effects. Metal oxides (including RuO_2, ZrO_2, CeO_2, TiO_2, and SnO_2,) have also been reported as co-catalysts added into Pt-based catalysts to achieve the same goals. However, adding a metal oxide may lead to poor electron conductivity, which may impair the function of the catalyst [48]. The results reported in literatures regarding binary catalysts confirm that these secondary metals are undeniably effective in improving catalytic activity. However, Pt–Ru still exhibits superior catalyst activity compared to other paired metals as an anode catalyst. However, researchers believe that Ru in Pt-based catalysts still demonstrates insufficient stability and activity and therefore, increased catalyst loading is required. To understand more about the methanol oxidation process in the DMFC system with a Pt-based alloy, Table 1 helps to interpret the mechanism. According to Neburchilov et al. [13], an effective approach in developing an anode catalyst for DMFCs is to accelerate all of the stages of methanol oxidation, including the rate-determining steps (RDSs). To accelerate

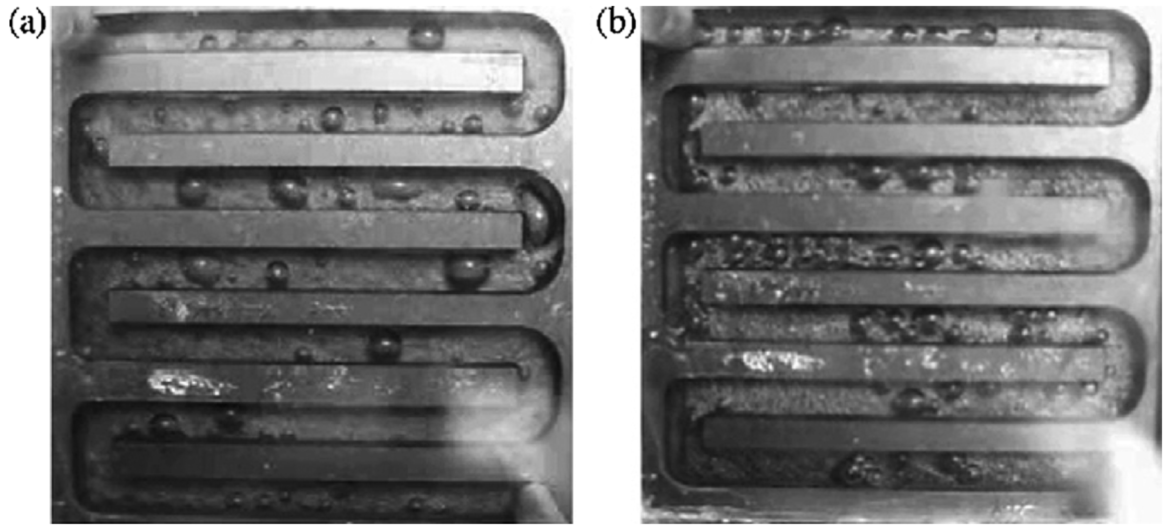


Fig. 12. Images of CO_2 bubble dynamics on the anodes with different microporous layers when the cell operating at 40 mA cm^{-2}, under application 2 mol L^{-1} methanol/oxygen, at 30 °C: (a) carbon black and 20 wt.% PTFE and (b) carbon black and 10 wt.% PTFE [42].

all of the stages of the methanol oxidation process at the anode, researchers found that the best combination was a Pt-based ternary or quaternary composition. Gurau et al. [49] mentioned that ternary and quaternary catalysts significantly improved catalytic performance. Ternary catalysts (Pt–Ru–Os, Pt–Ru–Sn, etc.) are considered to be the best combinations and strengthen the M—O bond, phase stability and help lower the potential for adsorption and activation of water, which satisfy the bifunctional model for methanol oxidation but lack effective C—H bond activation. The fourth metal, such as Ir or Rh, helps to overcome the deficiencies of C—H activation.

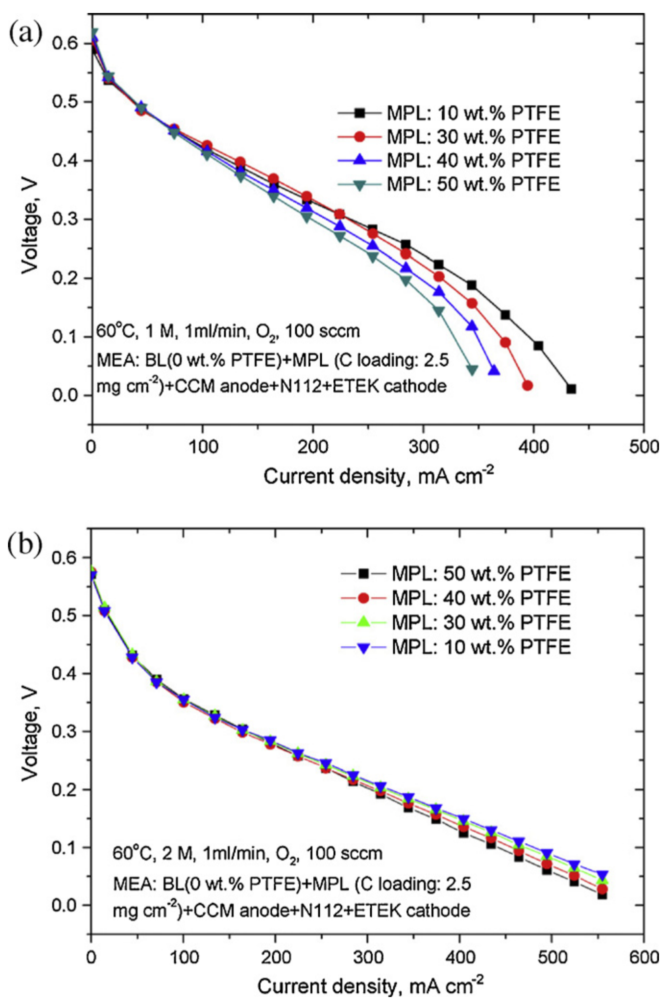


Fig. 13. Effect of PTFE loading in anode MPL on cell performance with (a) 1.0 M and (b) 2.0 M methanol operation [36].

As mentioned above, Pt was generally used as the catalyst at the cathode. Although Pt was generally used, its catalytic activity was still insufficient to obtain the required ideal ORR activity [50]. Oxygen does not dissociate on the Pt site. Therefore, the ideal ORR needs to occur with dissociated oxygen absorbed on the Pt-based catalyst to complete the four-electron reaction in DMFCs. Researchers have attempted to examine the binary and tertiary catalysts supported by carbon with various transitions metal, such as Pt–Fe, Pt–Cr, Pt–Ni, Pt–Co, and Pt–Cr–Co, and compared them to the Pt catalyst to improve ORR activity [17,51]. Baglio et al. [51] studied the performance of Pt-based binary catalysts with various transition metals. They found that Pt–Fe exhibited higher ORR activity and better performance than Pt. Fig. 14 shows the reaction activities for single cell DMFCs in the presence of transition metals in a cathode catalyst, which was able to complete the four-electron reaction. This proved that Pt demonstrated insufficient catalytic activity, which could be improved by the addition of a secondary or tertiary material. Besides ORR activity, the cathode catalyst also requires the use of materials to provide tolerance to methanol crossover. According

Table 1
Mechanism of the methanol oxidation process on Pt–M alloys, where M is the alloying component [13].

Methanol adsorption	
$Pt + CH_3OH \rightarrow Pt{-}(CH_3OH)_{ads}$	(1)
C—H bond activation	
$Pt{-}(CH_3OH)_{ads} \rightarrow Pt{-}(CH_3O)_{ads} + H^+ + e^-$	(2a)
$Pt{-}(CH_3O)_{ads} \rightarrow Pt{-}(CH_2O)_{ads} + H^+ + e^-$	(2b)
$Pt{-}(CH_2O)_{ads} \rightarrow Pt{-}(CHO)_{ads} + H^+ + e^-$	(2c)
$Pt{-}(CHO)_{ads} \rightarrow Pt{-}(CO)_{ads} + H^+ + e^-$	(2d)
Water adsorption (RDS)	
$M + H_2O \rightarrow M{-}(H_2O)_{ads}$	(3)
CO oxidation (RDS)	
$Pt{-}(CO)_{ads} + M{-}(H_2O)_{ads} \rightarrow Pt + M + CO_2 + 2H^+ + 2e^-$	(4)
Overall anode reaction	
$CH_3OH + H_2O \rightarrow CO_2 + 6H^+ + 6e^-$	(5)

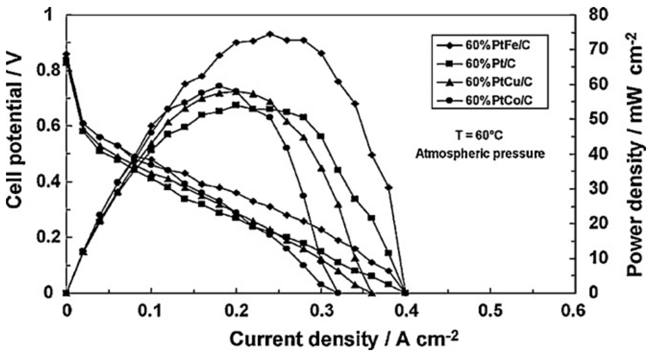


Fig. 14. Polarization and power density curves for the DMFCs equipped with the various cathode catalysts at 60 °C under atmospheric pressure [51].

to Li et al. [17] and You et al. [52], metals such as phthalocynines, porphyrins, metal oxides, metal carbides, ruthenium-based chalcogenides and macrocycles are among the most notable materials for this function because of their methanol tolerance. Although methanol tolerance on the cathode is greatly improved with these catalysts, these materials hardly reach the catalytic activity of Pt [52]. In addition, Pt also faces stability issues because of the dissolution of Pt particles. Researchers believe that high stability is necessary because the cathode catalysts are exposed to an acidic and oxidative atmosphere, which is a strong corrosive environment [50]. Zhai et al. [53] mentioned that Pt stability depends on a correlation between Pt particle sizes with the cell operating time (agglomeration) and dissolution and deposition of Pt in the polymer membrane. Ishihara et al. [50] found that non-precious metal oxides from Groups 4 and 5 were capable of providing sufficiently stable kinetics and high stability as the cathode catalyst layer. The solubility of the oxide-based catalyst in acid was lower than the Pt black as shown in Table 2. This demonstrated that the oxide-based catalysts were chemically stable. Even though oxide-based catalysts were kinetically and chemically stable, they exhibited insulating properties and poor ORR activity because of their large band-gap. Therefore more fundamental research is necessary to improve the catalytic activity for ORR.

According to Thiam et al. [54], usually, the use of nano-particles in catalysts and their morphologies depend on the catalyst support material, particle sizes and loading, which consequently influence the catalytic performance of the catalysts. In the past, several carbon materials have been tested as catalyst supports for DMFCs. The introduction of carbon with a high surface area to support the catalyst was a great effort to obtain good dispersion of nano-sized catalyst particles and to promote maximum performance while using the minimum amount of metal [55]. High surface area carbon blacks, such as Vulcan XC-72R, have been commonly used to enhance catalyst dispersion. Even though its high surface area (ca. 250 m^2/g) generally enhances catalyst dispersion, the presence of micropores (<2 nm diameter) in XC-72 plain carbon can induce poor catalyst utilization and mass transfer of reactants and products. The catalyst particles in the micropores are inaccessible to the methanol due to ionomer blockage (Fig. 15(a)), which occurs when the supported catalyst is mixed with the ionomer in the catalyst layer. Furthermore, the XC-72 carbon generally contains sulfur groups and may cause aggregation of the catalyst particles [56,57]. To enhance the catalyst utilization and increase the performance, Park et al. [57] modified the carbon support to extent the three phase boundaries and maximize the catalyst utilization in the catalyst layer. Fig. 15(b) and (c) shows a diagrammatic representation of the ionomer-coated carbon supports with modified carbon and modified carbon incorporated with catalyst particles, respectively, while Fig. 16 shows a TEM image of catalyst dispersion of the carbon-coated catalyst.

Table 2
Solubility of oxide-based catalysts in 0.1 mol dm^{-3} H_2SO_4 at 30 °C under atmospheric condition [50].

Catalyst	Solubility
TaOxNy (powder)	0.33
TaOxNy (thin film)	0.20
ZrOxNy (thin film)	0.041
TiO_{2-x} (plate)	0.36 (50 °C)
Pt black (powder)	0.56

Recently, there has been increased interest in adopting carbon nanostructure in novel catalyst supports to achieve high catalytic activity toward methanol oxidation and oxygen reduction [58]. Two types of CNT materials are commonly used: single-walled (SWCNTs) and multi-walled CNTs (MWCNTs), which consist of single and multiple graphite layers in the wall of the tube, respectively [59]. Several studies have revealed that CNTs were superior to carbon black as catalyst supports for DMFCs [56,59–61]. Chen et al. [61] observed that the type of carbon support material affected the morphology of the catalyst particles. TEM images of the catalysts on SWCNTs, MWCNTs and XC-72 show different morphological features (Fig. 17). Pt on XC-72 and MWCNTs demonstrates a spherical-shaped nanocatalyst, which is uniformly dispersed with slight agglomeration (only at MWCNTs) as shown in Fig. 17(a) and (b). For SWCNTs, the Pt particles demonstrate the unique needle-shaped morphology (Fig. 17(a)). Wu et al. [59] found that the catalyst particles on SWCNTs appeared to be in closer contact with the network of entangled and branched bundles of SWNTs compared to MWCNTs and XC-72 as the catalyst support in the presence of a binder (Fig. 18) and assumed shapes similar to highly exposed spheres. It is noteworthy that the Pt particles were anchored mainly at the boundaries of the SWCNT bundles and Nafion binders, which would be highly favorable in the transport of electrons and protons during electrocatalysis. Among the two types of CNTs as supporting carbon materials, SWCNTs significantly altered the morphology and the electronic structure of the catalyst nanoparticles due to their particular structures compared to MWCNTs and XC-72 [59]. Although catalyst nanoparticles on SWCNTs do not exhibit uniform particle distribution and demonstrate small average particle sizes, the results of the electro-catalytic activity of methanol oxidation characterized by cyclic voltammetry indicated that SWCNTs were an excellent catalyst supporting material with 12.1 mA cm^{-2} for Pt/SWCNTs, 7.8 mA cm^{-2} for Pt/MWCNTs and 6.9 mA cm^{-2} for the Pt/XC-72 catalyst as shown in Fig. 19.

Chiang and Ciou [62] showed the catalyst particle morphologies on different carbon supports (Fig. 20). Catalyst particles on oxide CNTs demonstrated smaller particles compared to pristine CNTs and exhibited superior dispersion compared to pristine CNTs and carbon black. Moreover, modification of the carbon support also improved mass transfer because the hydrophilic properties of the oxide-CNTs promoted good methanol delivery through the network structure formed by the CNTs.

In addition, CNTs can lead to reduction of the active surface area of the catalyst. CNTs normally possess outer diameters of 10–50 nm, inside diameters of 3–15 nm (pore size), and tube lengths of 10–50 nm. There is great possibility for catalyst nanoparticles depending on particle size to exist inside the nanotube, and the number of catalyst particles inside the tube increases as the tube length increases. These catalyst nanoparticles do not play a major role in the chemical reaction and lower the electrochemical activity due to the decreased surface area exposed to the reactants [34,63].

Another notable carbon nanostructure is the carbon nanofiber (CNF). Carbon nanofibers have unique structures, as mentioned in Section 3.1, and exhibit a highly electro-conductive graphite-like

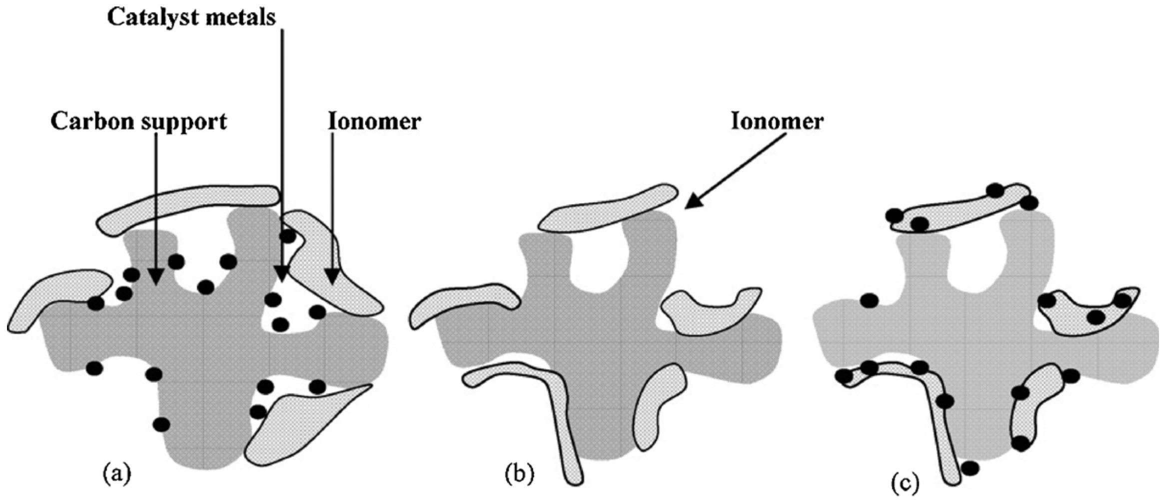


Fig. 15. Diagrammatic representation of: (a) catalyst–ionomer interaction in electrode using plain carbon as a support; (b) ionomer-coated carbon support; and (c) catalyst–ionomer interaction on ionomer-coated carbon support [57].

layer. Typically, CNFs can be divided into platelet CNFs (p-CNFs), tubular CNFs (t-CNFs) and fish-bone CNFs (f-CNFs) according to the different arrangements of the graphene layers as shown in Fig. 21 or in a schematic for easier understanding as shown in Fig. 22 [64]. Unlike CNTs, CNFs are non-microporous, which prevents the catalyst nanoparticles from being trapped inside. CNFs as catalyst supports were prepared for fuel cells, and their metal dispersion, morphologies and catalytic activity were compared to other carbon supports. Bessel et al. [65] employed Pt/CNFs and Pt/(Vulcan XC-72) as the electrocatalysts for direct methanol fuel cells (DMFCs) and found that p-CNFs and t-CNFs, which mainly exposed edge sites to the reactants, were superior to f-CNFs or Vulcan XC-72 in terms of ORR activity. The performance of CNFs tended to show inferior performance when the properties of the CNFs deviated as reported by Ismagilov et al. [66].

Guo et al. [58] mentioned that the existence of carboxyl groups on the surface of the CNFs significantly influenced the morphology and crystallinity of the electrocatalyst. They compared the oxidized (OCNFs) and reduced CNFs (RCNFs) as anode catalyst supports and found from TEM and XRD analyses that catalysts on RCNFs have smaller particle sizes and increased uniform distribution compared to the OCNFs, which tend to agglomerate due to the effects of functional groups. The morphologies of the catalysts on OCNFs and RCNFs are shown in Fig. 23. Similar to the o-CNTs, the OCNFs also furnish hydrophilic properties, which allow mass transportation to occur at the anode side through the network structure when catalyst/OCNFs are used the catalyst layer. In addition to the nanostructures discussed above, carbon nanocoils (CNC), carbon nanowires (CNW), and mesoporous carbon are also promising materials for use in catalyst supports. Park and Sung [67] found that CNC-supported catalysts exhibited improved performance compared to catalysts supported by Vulcan-X72 carbon.

As a catalyst layer, carbon nanostructures resulted in a smoother surface. The catalyst layer surface morphology with carbon nanostructures as a catalyst support will become denser compared to the MPL, which uses the same materials. This is a result of the binder effect and the hydrophobic properties added to the layer when the catalyst layer is prepared by the conventional ink process [68] and is spread by either a doctor blade, spraying, brushing or rolling (spreading methods influencing the morphology will be

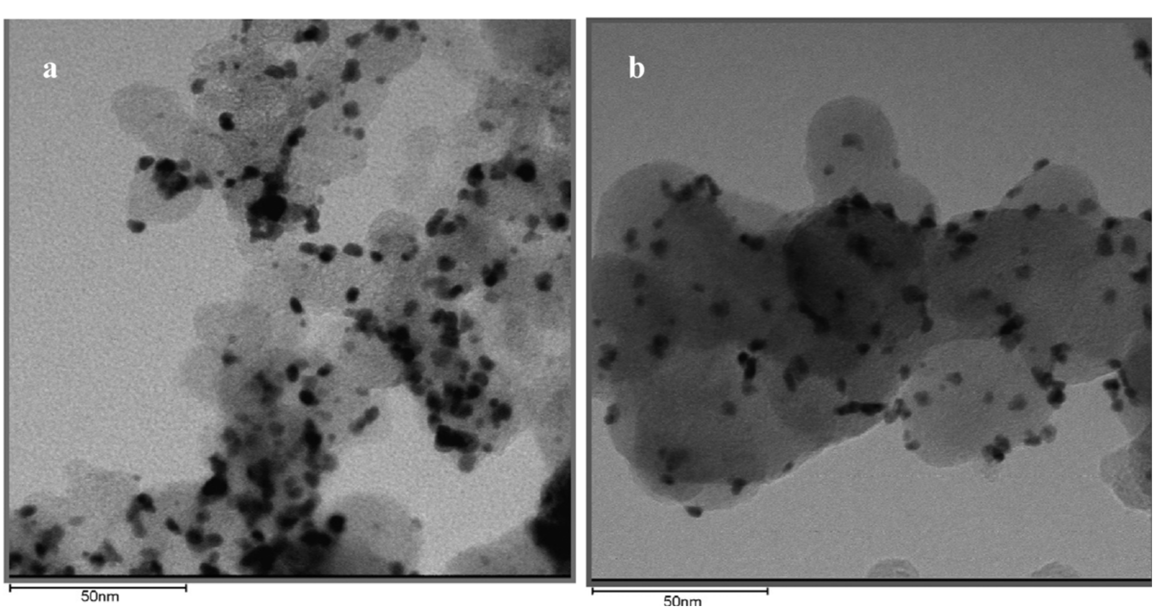


Fig. 16. Transmission electron micrographs of: (a) plain carbon and (b) modified carbon [57].

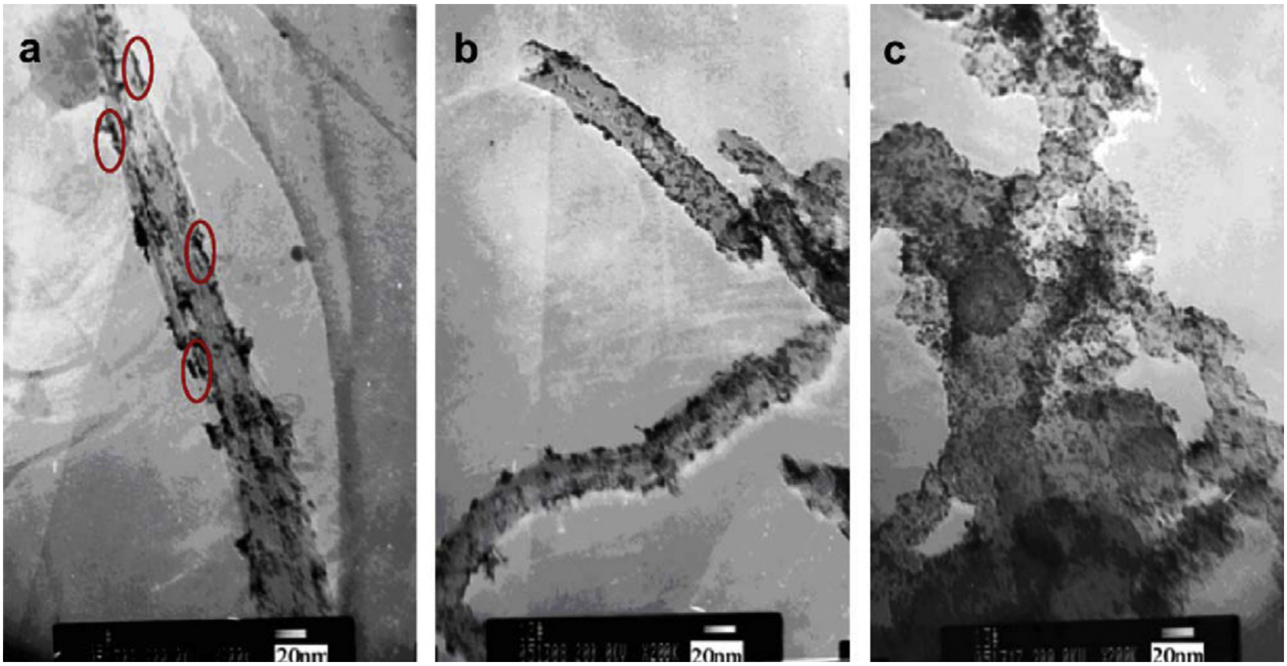


Fig. 17. TEM images of (a) Pt/SWNT, (b) Pt/MWNTs and (c) Pt/XC-72 catalysts [61].

discussed at the end of this topic) as shown in Fig. 24. These processes prevent the reactants from accessing the inner electro-catalyst sites and removing the products [69]. For these reasons, new structures were prepared by altering the layer preparation to increase the catalyst and pore distributions, mass transfer, catalyst utilization and electron conductivity [68,69]. Carbon nanostructures grown in situ on carbon substrates as integrated gas diffusion and catalyst layers demonstrate great potential for the

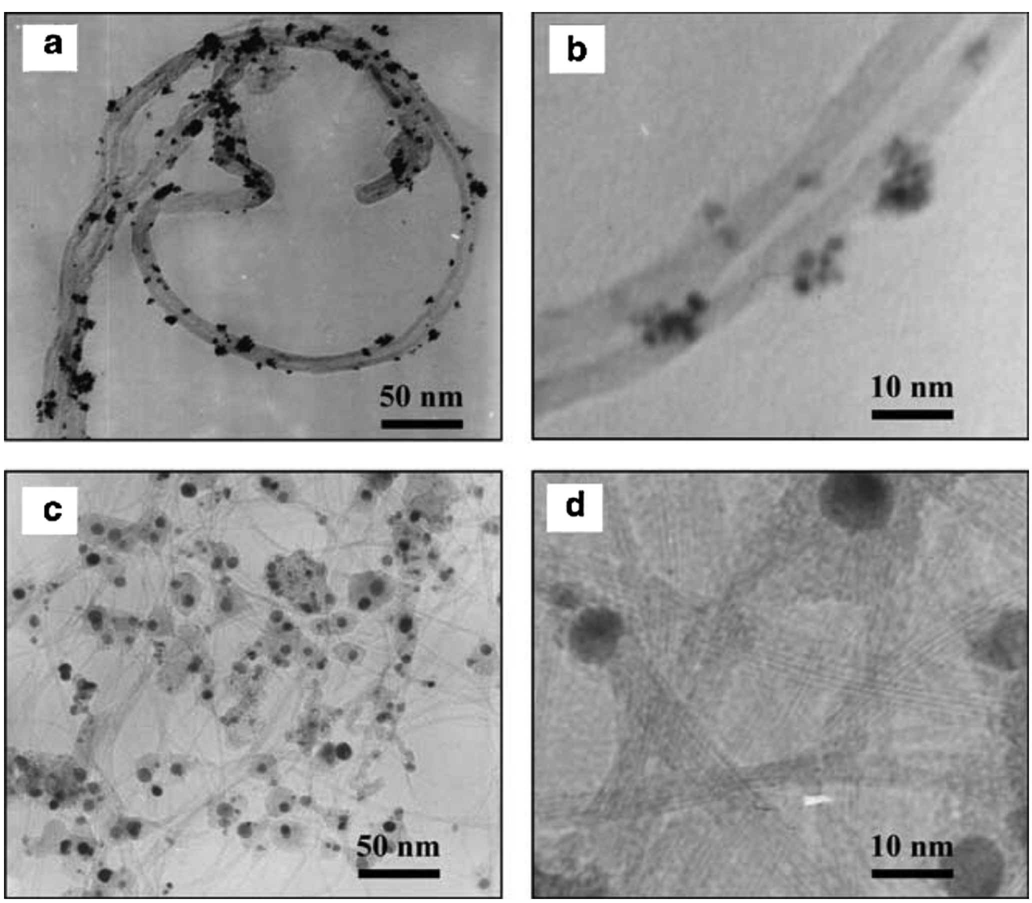


Fig. 18. TEM images of Pt-MWNT (a and b) and Pt-SWNT/Nafion (c and d) [56].

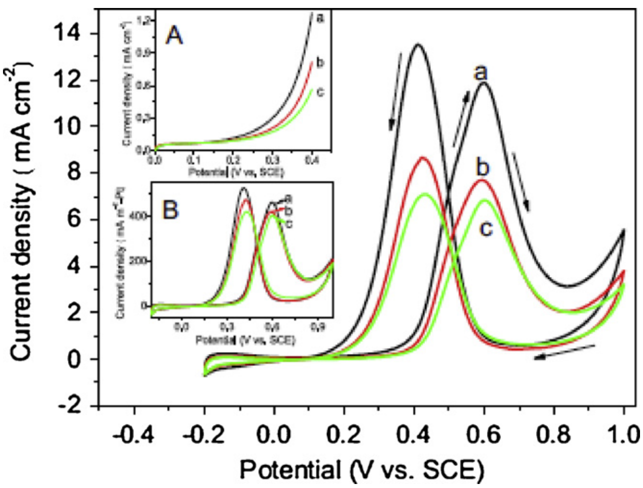


Fig. 19. Cyclic voltammograms of (a) the Pt/SWNTs, (b) the Pt/MWNTs and (c) the Pt/XC-72 catalysts in the 0.5 M H_2SO_4 D 0.5 M CH_3OH solutions at the rate of 50 mV s^{-1}. The inset (A) shows linear-sweep voltammograms in the potential range of 0–0.4 V; the inset (B) shows the CV curves normalized using the Pt surface area (mA m^{-2} Pt) [61].

improvement of electrode structure and configuration. Catalysts then deposit on the growing carbon nanostructure. Using this method, Tang et al. [70] found that the catalyst layer surface morphology (Fig. 25) exhibited uniform pore distribution and the structure provided enhanced catalyst utilization. Furthermore, electrochemical impedance spectroscopy (EIS) results (not shown here) confirmed that the carbon nanostructure layer grown in situ can provide both enhanced charge transfer and mass transport properties. This preparation method also seemed to be a promising way to prepare low-cost electrodes for DMFCs [69].

Catalyst loading in DMFC electrodes is also an important parameter to control because it is related to cell performance, electrode thickness, mass transfer and cost. Generally, compared to hydrogen-fueled polymer electrolyte fuel cells, DMFCs require a 10 times larger amount of catalyst loading, and in addition, more catalyst loading results in a more passive DMFC system than the active system [30]. Although high catalyst loading is required in DMFCs to achieve high power density, it also contributes to increased cost. Therefore, it is important to optimize the catalyst loading [72]. When the catalyst loading is increased, the active surface area of the electrode is also increased. Increasing the catalyst active site is beneficial because it reduces the activation overpotential. However, Bae et al. [71] and Zhao et al. [73] proclaimed the thickness of the catalyst layer also increases with catalyst loading, and the concentration overpotential increases due to mass transfer resistance throughout the thicker catalyst layer. At the anode, the concentration gradient for methanol becomes steeper with increasing electrode thickness and could yield excessive resistance against the methanol supply and carbon dioxide removal [71,73,74]. The interplay between a larger area of activation sites and supplying adequate methanol results in a balance between loading and performance behaviors [74]. Therefore, increasing the catalyst loading does not guarantee improved performance, and performance will reach a plateau or even decline with increasing catalyst loading [71].

Zhao et al. [73] examined the effect of catalyst loading at the anode site and found that when the thickness of the catalyst layer exceeded the "penetration depth", the electro-chemical reaction was predominantly taking place in the "inner" part of the catalyst layer, whereas the outer part was less active. Further increases in loading hindered methanol diffusion to reaction sites. Fig. 26 shows the impedance diagram from experimental work with different Pt–Ru loadings measured at a potential of 0.3 V (vs. DHE) in a half-cell configuration at 75 °C. The loops indicated the charge-transfer resistance, which was related to the methanol oxidation kinetics. As shown in Fig. 26, the size of the semicircle decreased with increasing catalyst loading, but when the catalyst loading increase above a certain level, the relationship disappeared. This

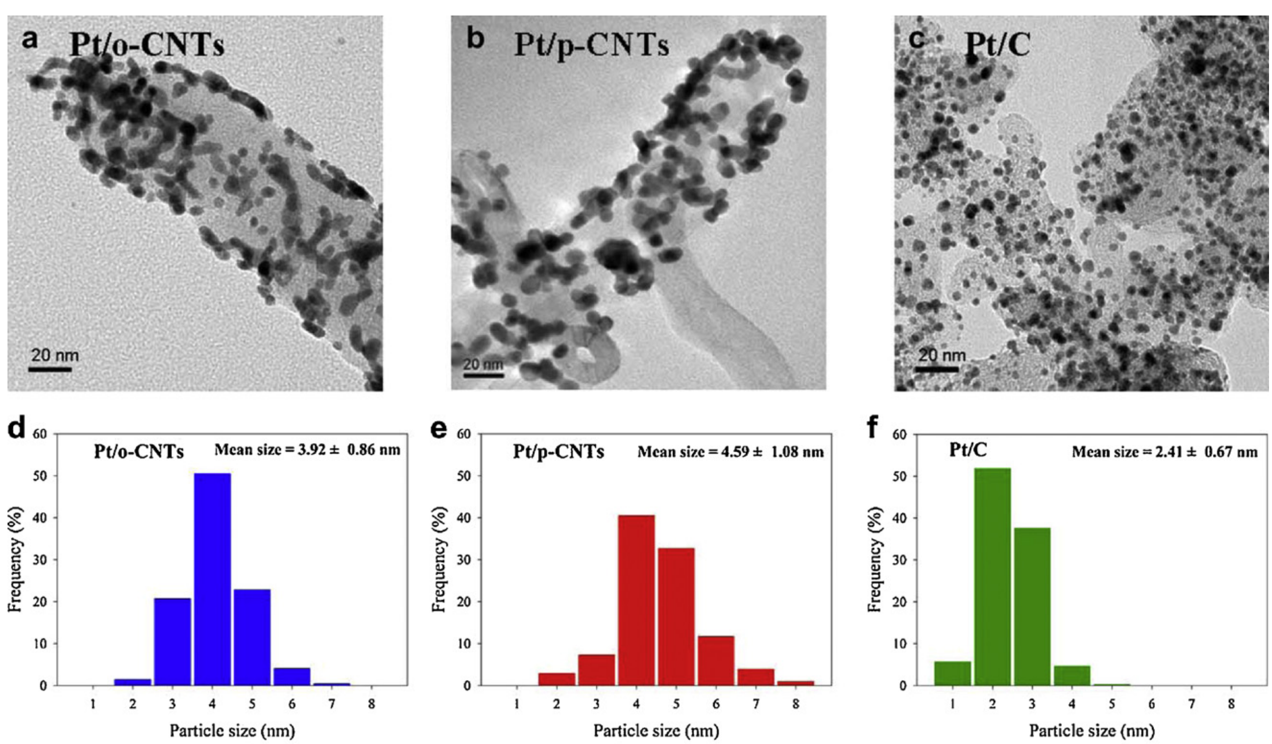


Fig. 20. HRTEM images and particle size distributions of (a and d) Pt/oxide-CNTs (Pt/o-CNTs); (b and e) Pt/pristine-CNTs (Pt/p-CNTs); and (c and f) Pt/Vulcan (Pt/C) (E-TEK) [62].

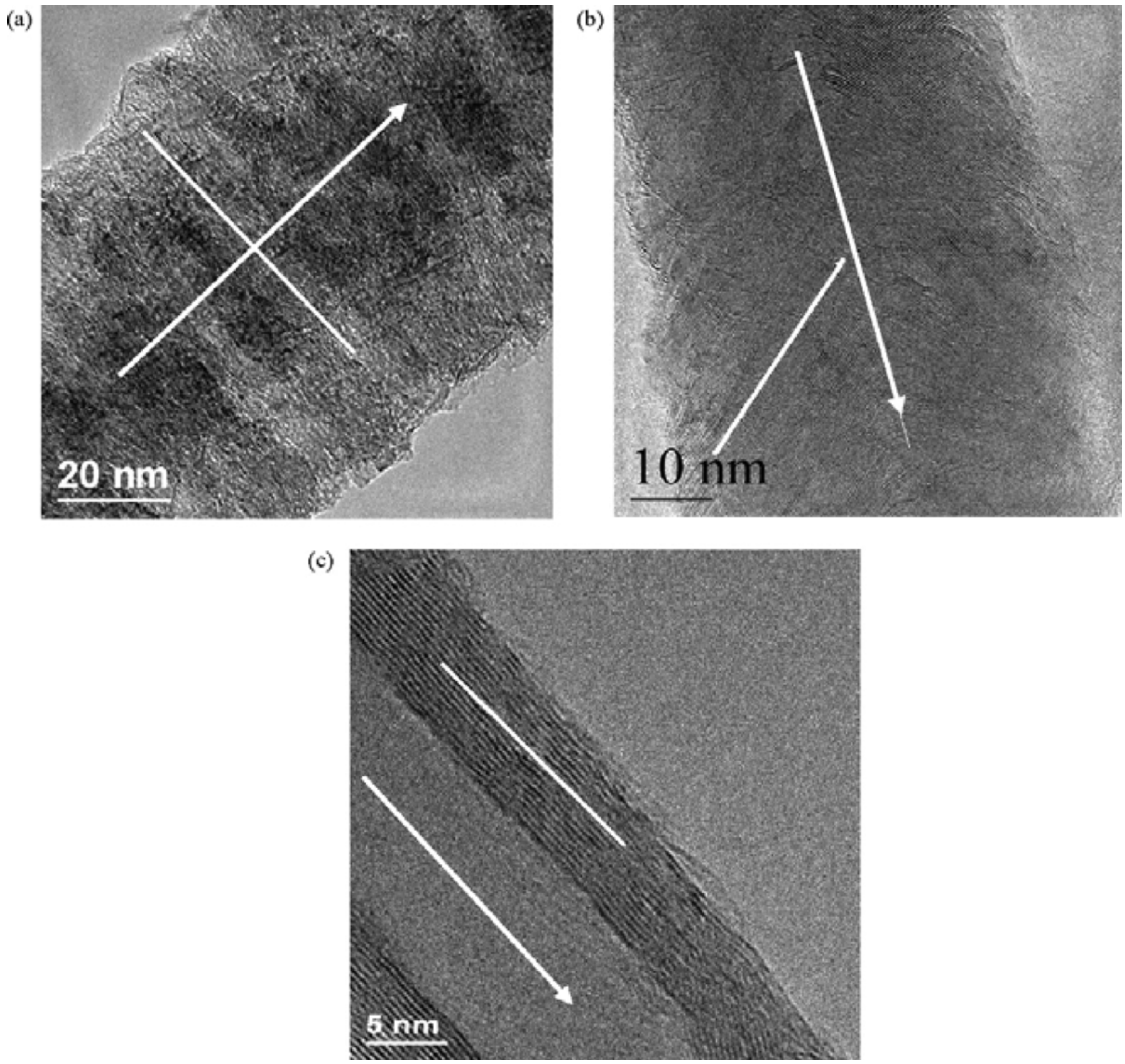


Fig. 21. HRTEM images of CNFs with different microstructures: (a) p-CNF, (b) f-CNF and (c) t-CNF [64].

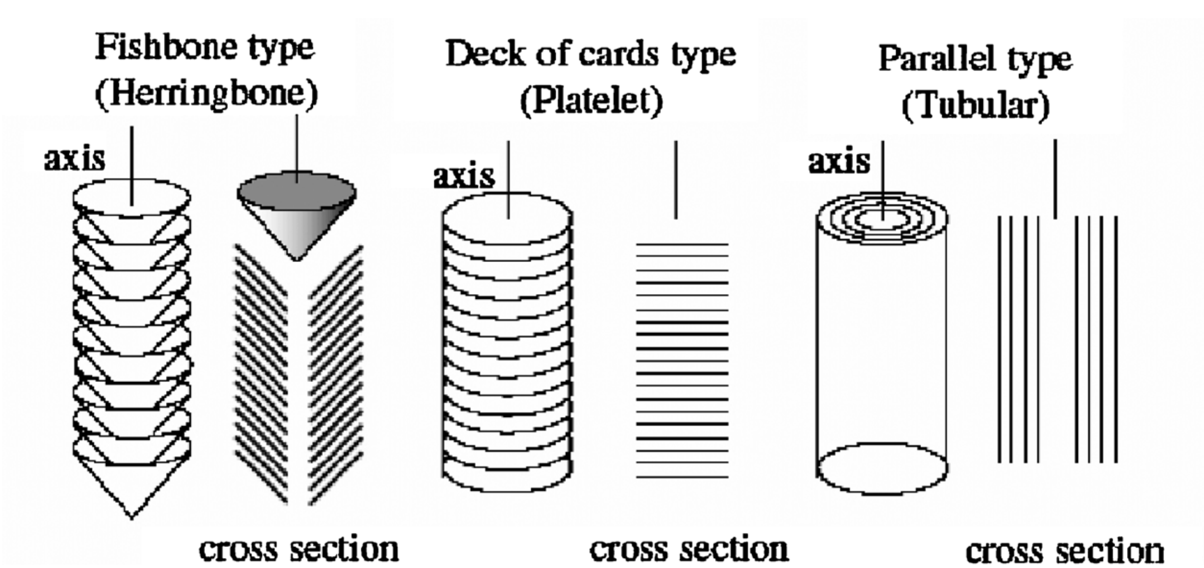


Fig. 22. Schematic representations of three types of CNFs [66].

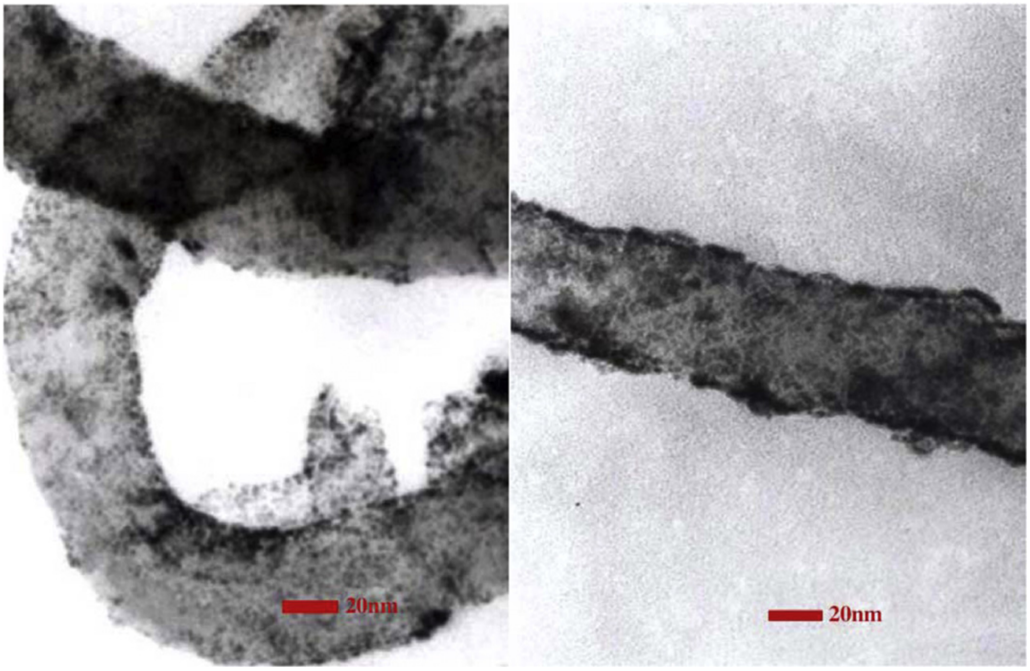


Fig. 23. TEM image of (a) PtRu/RCNFs and (b) PtRu/OCNFs [58].

occurred due to a thicker catalyst layer, which increased the transfer resistance. These results clearly demonstrated that finding the optimum catalyst loading is necessary to achieve high power output and eliminate the constraints related to it.

Another important parameter to consider in preparing an effective MEA is the ionomer content in the CL. The main functions of the ionomer is to build channels for ion transport to ensure efficient proton conduction between the reaction site and the membrane and to serves as a binder to hold the catalyst particles in the CL and between the CL membrane. Moreover, the ionomer also acts as a hydrophilic agent to retain moisture and to prevent membrane dehydration [75–77]. Nafion solution is among the popular ionomer materials widely used by researchers in DMFCs because it performs the main functions. Ionomer loading in the catalyst layer affects cell performance. Therefore, the optimum ionomer loading needs to be identified to maximize the performance. Low ionomer loading leads to poor conduction throughout the catalyst layer and may result in low adhesion strength between the CL and the membrane and between the catalyst particles. Meanwhile, high ionomer loading may result in a poor electrical connection between the catalyst particles, and the electrons may have a difficult time leaving [76].

The utilization of ionomers according to Abdelkareem et al. [75] varied depending on the preparation method, catalyst type, diffusion media and also the operating conditions. Catalyst layers produced on different substrates (i.e., decal sheets, gas diffusion layers or directly on membranes) resulted in different mass transport limitations. Non-porous and porous substrates required different ionomer contents. The non-porous substrate (normally used in the decal method) repelled the ionomer, while the porous media (i.e., a microporous layer (MPL), carbon paper or carbon cloth) allowed a large portion of the ionomer to permeate through

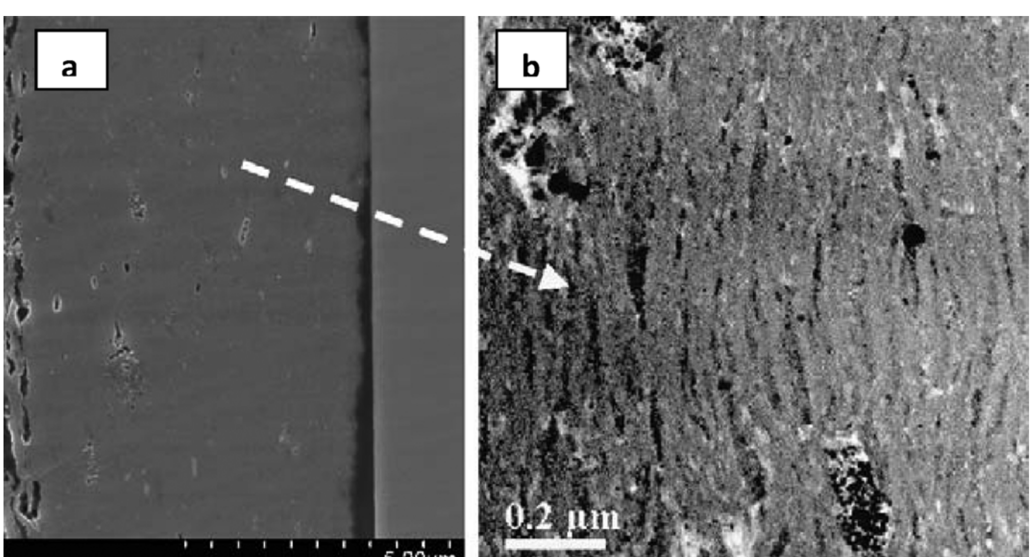


Fig. 24. Cross-section of catalyst layer (SEM), and (c) nano-structured catalyst supports catalyst layer (TEM) [68].

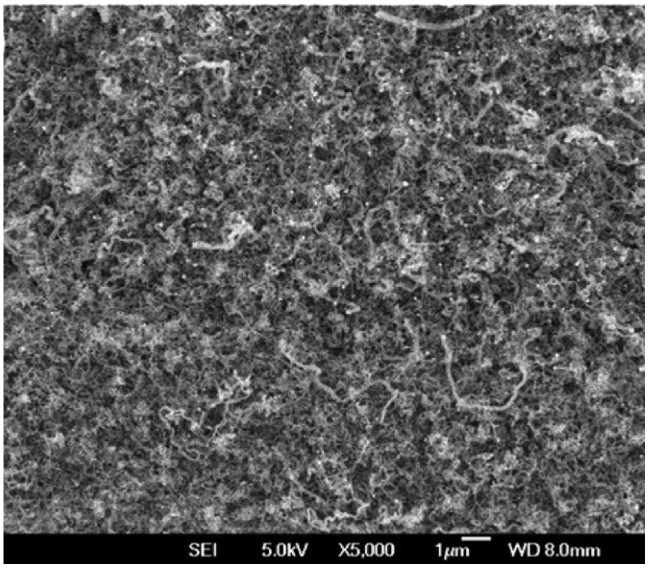


Fig. 25. SEM image of CNTs grown on carbon paper and catalyst particle deposited via sputter deposition [70].

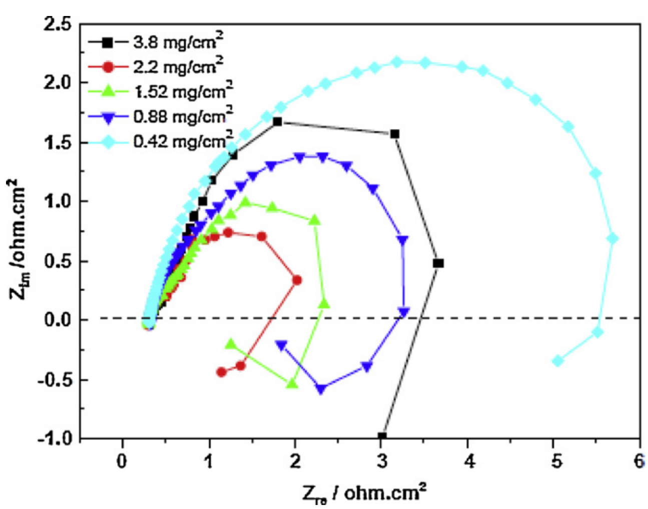


Fig. 26. Anode impedance spectra with different Pt–Ru loading [73].

the layer. Therefore, different optimum ionomer contents have been reported by researchers based on different preparation methods as shown in Table 3. Around 7–15 wt.% is required in the decal method, while other methods require a higher percentage to achieve an optimum ionomer content. Jeng et al. [78] mentioned if the preparation was performed under vacuum, more ionomer was lost by permeation, and a higher ionomer concentration was required.

Lee et al. [83] revealed that another issue with the ionomer is the compatibility between the membrane and the ionomer in the catalyst layer. Incompatibility between the polymeric membrane and the ionomer in the catalyst layer can lead to high interfacial resistance and performance losses in fuel cells. Pairing the ionomer and membrane with the same basic materials can counter the incompatibility problem while lowering the interfacial resistance and controlling the fuel loss in DMFCs.

There are several ways to spread the catalyst onto the GDL (carbon cloth or carbon paper). Brushing, spraying, casting and rolling were among the techniques used by researchers in preparing the electrodes. Each method for preparing the catalyst layers on the GDL resulted in different surface morphologies. Wang et al. [10] investigated the relationships between morphology and electrochemical behaviors. They prepared three different morphologies via three different catalyst preparing methods. Using brushes, spray guns and rollers to prepare the catalyst layers, they found that each method produced different surface morphologies. Fig. 27 shows SEM image of three different preparing methods. The catalyst layer faces several problems, such as cracks and uneven surfaces.

Choi et al. [84] also investigated the effects of various coating methods on the performance of the cells. They evaluated the differences among three different spray methods, namely air-spray, electro-spray and dual-mode spray. They found that the catalyst agglomerated in all three methods, but the sizes of the agglomerates were different among all of the methods. Dual-mode spray, as shown in Fig. 28(a), demonstrated the best morphology with smaller sizes of particle agglomerates and increased porosity. The FE-SEM images in Fig. 28 show the structures of three different methods. Dual-mode spray produced smaller and more uniform particles. This created an advantage over the other two methods because it leads to a larger electrochemically active surface (EAS) and improved DMFC performance.

3.3. Membrane

Nafion membranes are the most widely used and studied PEM materials in fuel cells because of their unique properties, including their high proton conductivity (≈0.1 S/cm), good mechanical strength and chemical stability in a fully hydrated state. Several major drawbacks of the Nafion membranes in DMFCs include a dependence on water content limits [21] and methanol crossovers, which allow methanol move across the membrane to the cathode side [85–87]. The permeated methanol is chemically oxidized to CO_2 and H_2O at the cathode, which decreases the fuel efficiency and depolarizes the cathode. Permeated methanol can also adversely affect the cathode performance due to the consumption of oxygen through methanol oxidation at the cathode catalyst layer, which lowers the oxidant activity in the cathode side of the cell [22]. For these reasons, researchers focused on the development of an alternative thermoplastics polymer for use in the electrolyte membrane such as poly(etheretherketone) (PEEK) [88,89], polysulfone (PSF) [90,91] and polybenzimidazole (PBI) [92], which all exhibit strong chemical stability. These materials need to be chemically stable and mechanically strong, impermeable to fuel and effective at mediating proton transport. Therefore,

Table 3
List of the previous studies that investigated the optimum ionomer content in the catalyst layer for the DMFC.

No.	Preparation method	Operation mode	Opt. Nafion content (wt.%)		Ref.
			Anode	Cathode	
1	Decal/CCM	Active	15	-	Zhao et al. [73]
2	C cloth, MPL sedimentation using micropipette	Passive	20	20	Abdelkareem et al. [75]
3	Decal	Active	7	–	Dohle et al. [79]
4	C cloth, vacuum filtration	Active	63	–	Jeng et al. [78]
5	C paper treated	Active	36	–	Chu et al. [81]
6	C paper, spraying	Active	45.4	45.4	Bunazawa et al. [82]

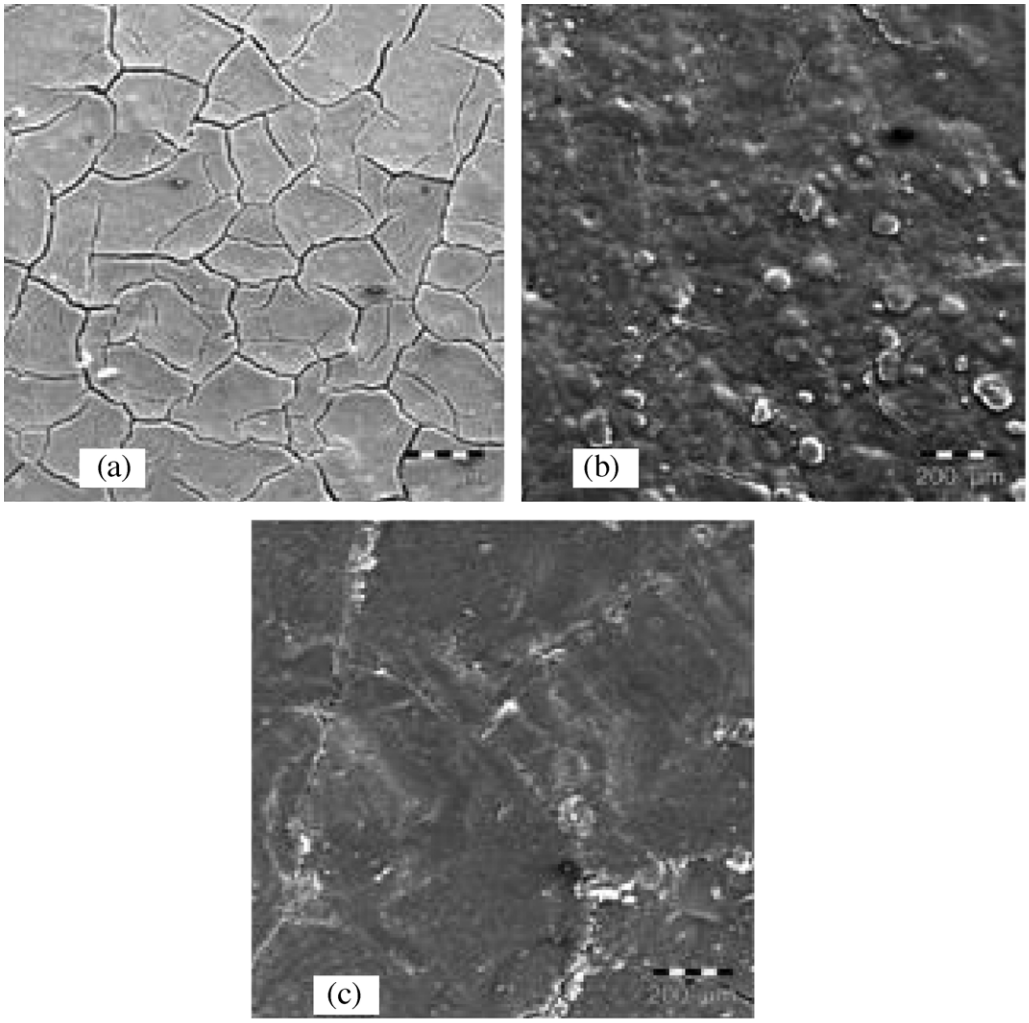


Fig. 27. SEM micrographs of: (a) brush, (b) spray, and (c) roll [10].

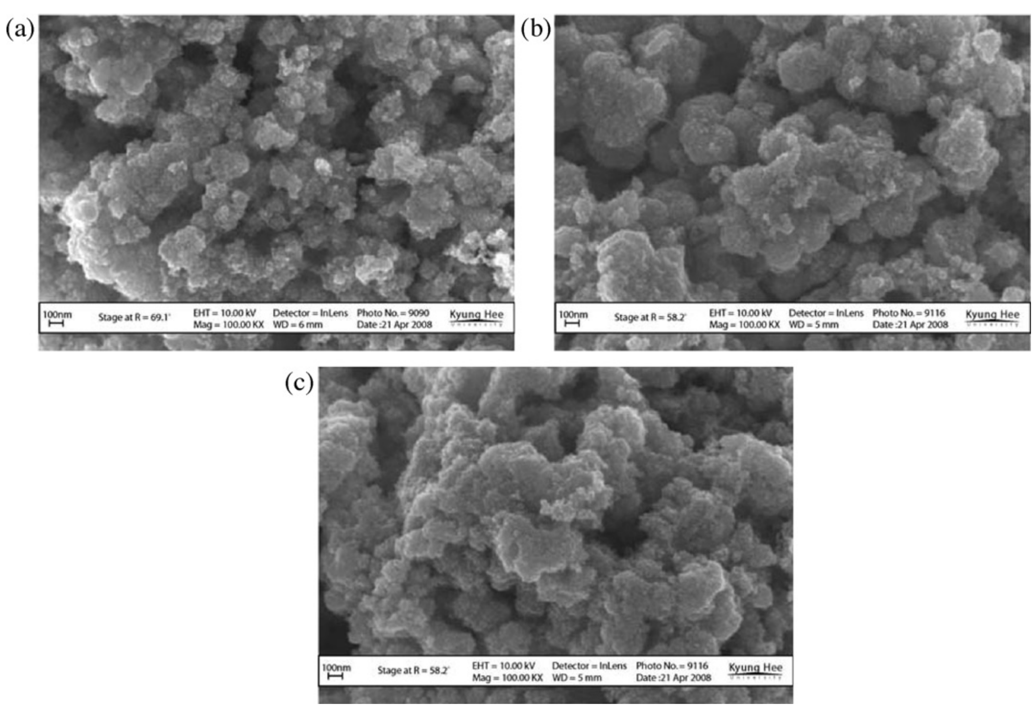


Fig. 28. FE-SEM images of catalysts on electrodes coated by: (a) dual-mode spray, (b) electro-spray, and (c) air-spray [84].

fine tuning of the molecular structure is needed to achieve the best combination by attaching the sulfonic groups to the polymer chains, which are physically cross-linked by non-sulfonated regions and are usually more hydrophobic [69]. Sulfonation of polymers improves their membrane properties in terms of better wettability, higher water flux, higher antifouling capacity, better selectivity, and increased solubility in the solvent for processing [93]. This thermoplastic sulfonated polymer membrane has been considered to be one of the best alternatives because it offers the attributes of adjustable proton conductivity, excellent chemical stability, hydrophobic–hydrophilic balance and thermal stability [21,22]. Xing et al. [93] investigated the sulfonation of PEEK and found that adding sulfonic groups to the polymer chains increased the conductivities of the SPEEKs with increasing degrees of sulfonation (DS).

The composite membranes were mostly prepared by addition of a nonconductive ceramic oxide such as silica, zirconia, and titania and less proton-conductive materials such as sulfonated montmorillonite and sulfonated phenethyl-silica [94]. The additional materials have been adapted to reduce fuel crossover and improve their water sustainability, morphologies, sizes, properties, and distributions [95]. In an investigation by Ren et al. [94], a combination of silica with Nafion as an organic/inorganic membrane for DMFC showed an approximately 50% decrease of methanol crossover compared with the commercial Nafion 117 membrane. They prepared the hybrid silica/Nafion membrane with various additives including $HS(CH_2)3CH_3Si(OCH_3)_2$ (SH—), tetraethyl orthosilicate (TEOS) and $HS(CH_2)_3CH_3Si(OCH_3)_2$-TEOS (HS-TEOS) in Nafion solutions. Kim and Chang [95] prepared the organic/inorganic hybrid membrane with silica supported by heteropoly acid. They observed an approximately 50–80% decrease in methanol crossover and a nearly 10% increase in fuel efficiency compare to the Nafion membrane. Fig. 29 shows an example of the hybrid membrane images captured by SEM.

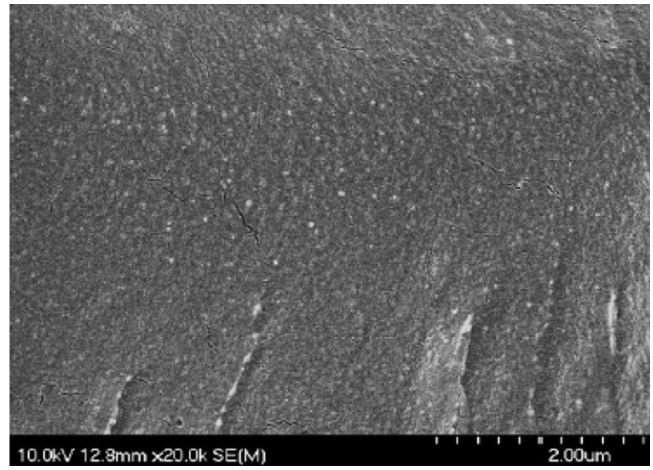


Fig. 29. SEM images of hybrid Nafion-based membrane [95].

Umeda et al. [80] prepared a hybrid, non-Nafion-based membrane from aromatic derivatives of methoxysilane and ethyl 2-[3-(dihydroxyphosphoryl)-2-oxapropyl]acrylate (EPA). Fig. 30 shows the possible structures of the hybrid membrane for both aromatic derivatives. Both hybrid membranes demonstrated different properties according to the siloxane linkages (Si—O—Si) formed, while the MDMSMS(D)/EPA showed higher chemical stability and mechanical properties. The higher conductivity of the DMMSMS(M)/EPA membrane was attributed to the larger amount of water in the membrane. They also claimed that the MDMSMS(D)/EPA hybrid membrane-based MEA retained high performance at temperatures reaching 100 °C in a fully humidified environment due to its high mechanical property. The MEA also exhibited good stability during fuel cell operation at 80 °C for at least 48 h. However, one of the challenges in the development of nano-structured membranes is the synthesis process, which always requires understanding of the fundamentals of nano-scale chemistry, physics and manufacturing methods to produce a homogeneous nanoparticle-enhanced membrane [96].

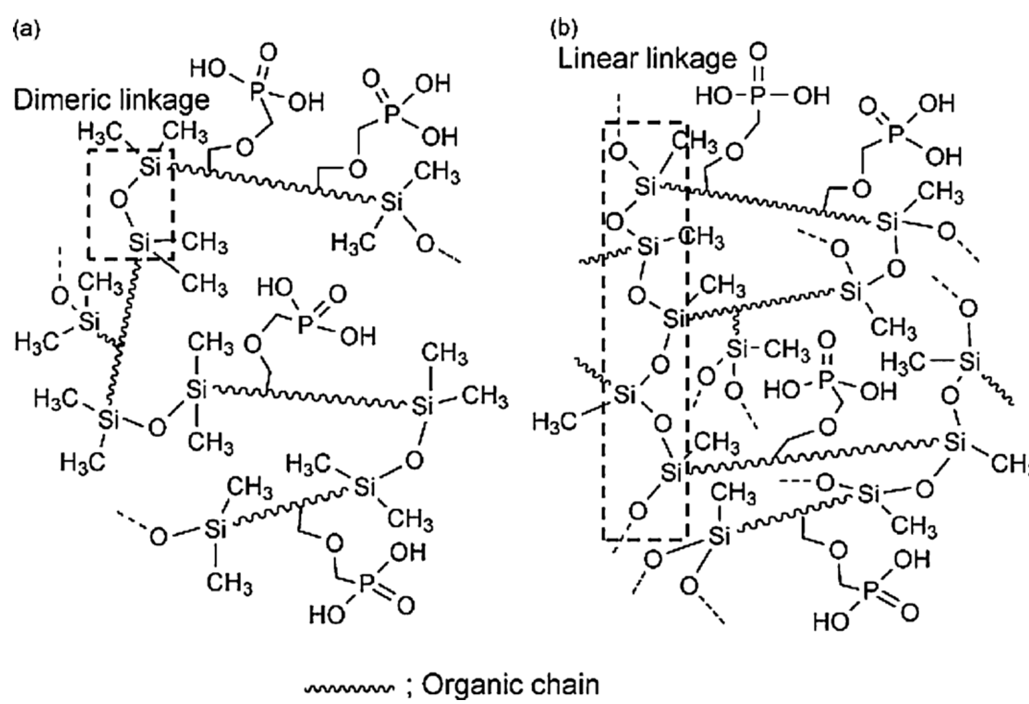


Fig. 30. Possible structures of hybrid membranes: (a) membrane from monofunctional DMMSMS(M)/EPA and (b) membrane from difunctional MDMSMS(D)/EPA [80].

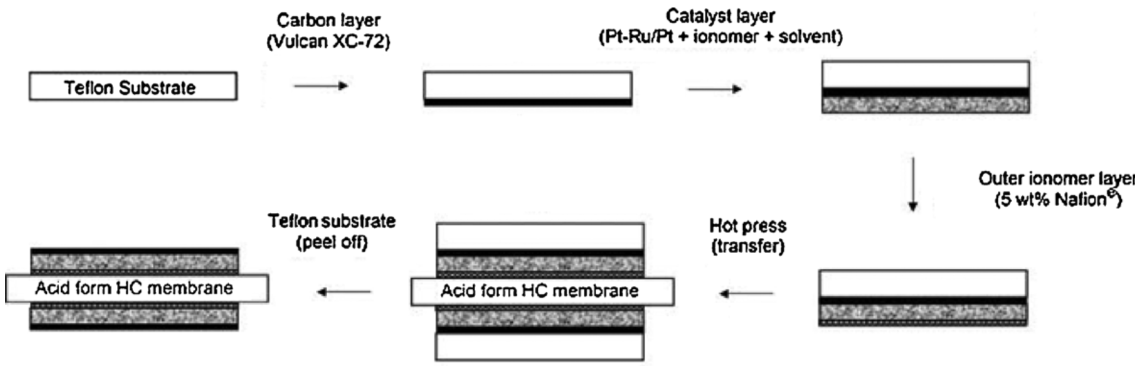


Fig. 31. Schematic representation of decal method fabrication for MEA [102].

4. MEA fabrication

In fabricating a unit of MEA, the interface membrane and catalyst layers must achieve the triple boundaries, in which the catalyst layer, electrolytes and reactants must be in close contact [97,98]. Therefore, MEA fabrication must meet this requirement to provide a large interface between those boundaries. Common and conventional methods used by many researchers to fabricate the MEA include hot pressing using a hot press machine [10,84,99] and pressing the catalyst-coated-substrate (CCS) with a membrane in the middle. This method is widely used in fabricating the MEA for PEMFCs [100,101]. This method requires the electrode to be prepared by applying a catalyst ink on the GDL as a substrate either by brushing, spraying or using a doctor blade. The membranes were placed between the anode and cathode electrodes and pressed at a high pressure and a high temperature for a specified time to form an integrally bonded unit.

Another method in fabricating the MEA is by producing a catalyst-coated-membrane (CCM). The CCM fabricating procedure is performed by spraying the catalyst ink directly onto the membrane surface. In this CCM method, spraying the wet ink onto the membrane directly will possibly swell and/or shrink the membrane [102]. To avoid this, the decal method was introduced to transfer the catalyst layer onto the membrane with a decal substrate. Fig. 31 represents a schematic step for the decal method in fabricating the MEA. In this decal method, carbon ink, catalyst ink

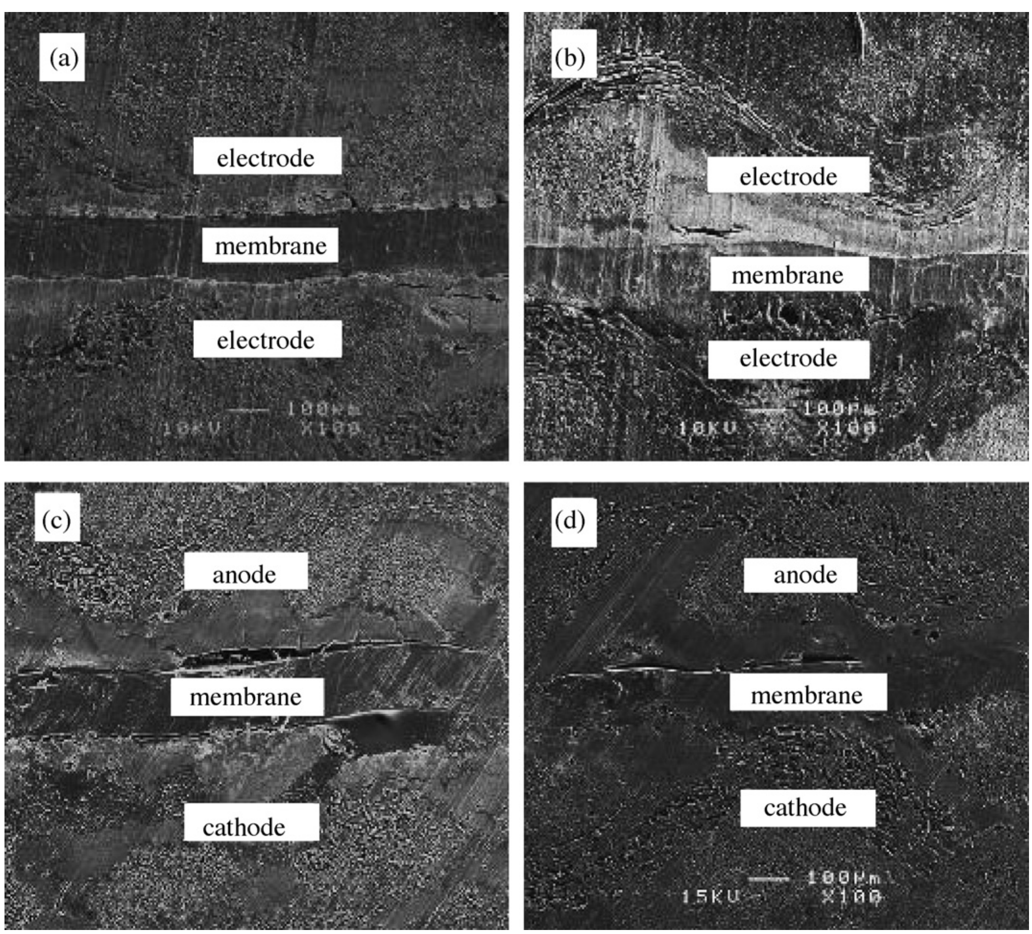


Fig. 32. SEM images of the G-MEA and C-MEA before and after conducting lifetime tests: (a) fresh C-MEA, (b) fresh G-MEA, (c) C-MEA after the lifetime test, and (d) G-MEA after the lifetime test [97].

and a Nafion solution were first transferred onto the support layer (Teflon film) individually to form a complete electrode layer. The electrode layer was then transferred to the membrane directly by hot pressing under high pressure and temperature for a specific time. The Teflon film support was then peeled away. To transfer each layer onto a Teflon film, a brushing or spraying technique was used to obtain a uniformly layer [103]. A backing layer was then placed on the anode and cathode sides of the CCM to form the full cell.

From the previous findings, researchers such as Wang et al. [98], Krishnan et al. [102] and Tang et al. [103] have investigated the MEA fabrication processes using the CCM, CCS (conventional hot pressing method) and CCM (decal method). They agreed the DMFC with decal method shows better performance compared to others and meet the commercial purpose of the DMFC. CCM using decal substrate shows improvements to DMFC performance due to the significantly higher electrochemical reaction sites and the increased three-phase boundaries through the reduction in the loss of the electrocatalysts in the gas diffusion layers and enhanced electrode–membrane interface.

The glue method for fabricating membrane electrodes was also proposed by a researcher. Liang et al. [97] found that by using this method, the cell performance was more stable than the conventional hot pressing method. They also found that the glue method was able to reduce the delamination problem after extended operation. Fig. 32 shows SEM images of the delamination problem after a life-time test for an MEA fabricated by the glue method (G-MEA) and an MEA fabricated using the conventional hot pressing method (C-MEA).

Pressure, temperature and time seemed to be important parameters in all of the MEA fabrication methods. Every method uses a certain pressure, temperature and time in the hot pressing step. These three parameters in the hot pressing step result in several effects on the MEA and the performance of the cell [25,27]. It is well known that hot pressing is a simple way to assemble the anode, cathode and membrane because it provides good interfacial contact between the electrodes and membrane. However, Song and Pickup [27] mentioned that the good interfacial contact was not the only characteristic needed for an effective MEA. The capability to maintain inner structural integrity and provide good porosity and performance after hot pressing is necessary because those aspects can be changed during the hot pressing process. Moreover, it also can cause the dehydration of the Nafion membrane, which may lead to an irreversible loss of performance of the MEA if the temperature and time for the hot pressing process are not optimized.

5. Conclusion

The MEA consists of a GDL, CL and a membrane. In engineering the MEA for fuel cells, materials, structures and layer morphologies are critical components that accelerate the reactions and transportations. Material selection is the key to determine the behavior and function of the layers. The GDL is formed by the BL and MPL. Carbon paper and carbon cloth are commonly used as BL materials; however, because of their fragile characteristics, metal fiber is a more promising material because of its high mechanical strength and ability to maintain porosity under various pressure conditions. However, metal fibers require tuning to match the functions according to the anode and cathode conditions. For the MPL, carbon nanostructures such as CNTs and CNFs are promising materials compared to carbon black in preparing a crack-free layer with uniform pore distribution and a continuous network that can enhance mass transfer, catalyst utilization and electron conductivity. Carbon nanostructures also provide smooth surfaces, which reduce the contact layer resistance.

To increase the catalyst activity, tertiary or quaternary components seem to be more promising. However, because of the high cost of certain metals, the non-precious catalysts are considered among the most promising catalyst materials, but they require further studies to increase performance. The structure and morphology of the catalyst layer are influenced mostly by the catalyst support materials. Among the carbon-based materials, carbon nanostructures provide the largest surface areas and thereby increase the catalytic activity. Catalyst layer structures built from carbon nanostructures provide increased mass transfer and electron conductivity compared to carbon black. Multi-component membranes help to alter the membrane structure. Compared to single-component membranes, the multi-component membranes cause an 80% reduction in methanol crossover and an approximate 10% increase in fuel efficiency. In addition, the introduction of nano-scale materials helps to enhance the interaction, reduce methanol crossover, improve the mechanical properties and increase the chemical stability. Smoother membrane surface morphology is achieved by using nano-scale materials, which improves interlayer contact between the membrane and catalyst layers. Therefore, in fabricating a highly effective MEA, the optimization of the structure and morphology of the layers is important not only in ensuring efficient mass transfer and electron and proton conductivity but also in reducing interlayer resistance.

Acknowledgment

The authors gratefully acknowledge the financial support of this work by the Malaysian Ministry of Science, Technology and Innovation (MOSTI) under the Research University Grant No. UKM-GUP-BTT-07-30-192 and UKM-AP-TK-08-2010.

References

[1] Kamarudin SK, Achmad F, Daud WRW. Overview on the application of direct methanol fuel cell (DMFC) for portable electronic devices. International Journal of Hydrogen Energy 2009;34:6902–16.
[2] Basri S, Kamarudin SK, Daud WRW, Ahmad MM. Non-linear optimization of passive direct methanol fuel cell (DMFC). International Journal of Hydrogen Energy 2010;35(4):1759–68.
[3] Hashim N, Kamarudin SK, Daud WRW. Design, fabrication and testing of a PMMA-based passive single cell and a multi-cell stack micro DMFC. International Journal of Hydrogen Energy 2009;34(19):8263–9.
[4] Xu C, Zhao TS, Ye Q. Effect of anode backing layer on the cell performance of a direct methanol fuel cell. Electrochimica Acta 2006;51:5524–31.
[5] Huang YF, Kannan AM, Chang CS, Lin CW. Development of gas diffusion electrodes for low relative humidity proton exchange membrane fuel cells. International Journal of Hydrogen Energy 2011;36:2213–20.
[6] Möst M, Rzepka M, Stimming U. Analysis of the diffusive mass transport in the anode side porous backing layer of a direct methanol fuel cell. Journal of Power Sources 2009;191:456–64.
[7] Park S, Popov BN. Effect of a GDL based on carbon paper or carbon cloth on PEM fuel cell performance. Fuel 2011;90:436–40.
[8] Xu C, Zhao TS, He YL. Effect of cathode gas diffusion layer on water transport and cell performance in direct methanol fuel cells. Journal of Power Sources 2007;171:268–74.
[9] Krishnamurthy B, Deepalochani S. Effect of PTFE content on the performance of a direct methanol fuel cell. International Journal of Hydrogen Energy 2009;34:446–52.
[10] Wang Z, Liu Y, Linkov VM. The influence of catalyst layer morphology on the electrochemical performance of DMFC anode. Journal of Power Sources 2006;160:326–33.
[11] Hogarth MP, Ralph TR. Catalysis for low temperature fuel cells. Platinum Metals Review 2002;46(4):146–64.
[12] Chen S, Ye F, Lin W. Effect of operating conditions on the performance of a direct methanol fuel cell with PtRuMo/CNTs as anode catalyst. International Journal of Hydrogen Energy 2010;35:8225–33.
[13] Neburchilov V, Wang H, Zhang J. Low Pt content Pt–Ru–Ir–Sn quaternary catalysts for anodic methanol oxidation in DMFC. Electrochemistry Communications 2007;9:1788–92.
[14] Lizcano-Valbuena WH, Paganin VA, Leite CAP, Galembeck F, Gonzalez ER. Catalysts for DMFC: relation between morphology and electrochemical performance. Electrochimica Acta 2003;48:3869–78.
[15] Caillard A, Coutanceau C, Brault P, Mathias J, Léger J-M. Structure of Pt/C and PtRu/C catalytic layers prepared by plasma sputtering and electric

performance in direct methanol fuel cells (DMFC). Journal of Power Sources 2006;162:66–73.
[16] Antoine O, Bultel Y, Ozil P, Durand R. Catalyst gradient for cathode active layer of proton exchange membrane fuel cell. Electrochimica Acta 2000;45:4493–500.
[17] Li W, Zhou W, Li H, Zhou Z, Zhou B, Sun G, et al. Nano-stuctured Pt–Fe/C as cathode catalyst in direct methanol fuel cell. Electrochimica Acta 2004;49:1045–55.
[18] Colón-Mercado HR, Popov BN. Stability of platinum based alloy cathode catalysts in PEM fuel cells. Journal of Power Sources 2006;155:253–63.
[19] Silva VS, Mendes AM, Madeira LM, Nunes SP. Membranes for direct methanol fuel cell applications: Analysis based on characterization, experimentation and modeling. In: Zhang XW, editor. Advances in fuel cells. Trivandrum, Kerala, India: Research Signpost 37/661 (2); 2005.
[20] Ahmad H, Kamarudin SK, Hasran UA, Daud WRW. Overview of hybrid membranes for direct-methanol fuel-cell applications. International Journal of Hydrogen Energy 2010;35:2160–75.
[21] Yang T. Composite membrane of sulfonated poly(ether ether ketone) and sulfated poly(vinyl alcohol) for use in direct methanol fuel cells. Journal of Membrane Science 2009;342:221–6.
[22] Silva VS, Mendes A, Madeira LM, Nunes SP. Proton exchange membranes for direct methanol fuel cells: properties critical study concerning methanol crossover and proton conductivity. Journal of Membrane Science 2006;276:126–34.
[23] Park S, Lee JW, Popov BN. Effect of carbon loading in microporous layer on PEM fuel cell performance. Journal of Power Sources 2006;163:357–63.
[24] Liu J, Sun G, Zhao F, Wang G, Zhao G, Chen L, et al. Study of sintered stainless steel fiber felt as gas diffusion backing in air-breathing DMFC. Journal of Power Sources 2004;133:175–80.
[25] Zhang J, Yin GP, Wang ZB, Lai QZ, Cai KD. Effects of hot pressing conditions on the performances of MEAs for direct methanol fuel cells. Journal of Power Sources 2007;165:73–81.
[26] Nakagawa N, Sekimoto K, Masdar MS, Noda R. Reaction analysis of a direct methanol fuel cell employing a porous carbon plate operated at high methanol concentrations. Journal Power Sources 2009;186:45–51.
[27] Song C, Pickup PG. Effect of hot pressing on the performance of direct methanol fuel cells. Journal of Applied Electrochemistry 2004;34: 1065–70.
[28] Liu C, Xue X, Lu T, Xing W. The preparation of high activity DMFC Pt/C electrocatalysts using a pre-precipitation method. Journal of Power Sources 2006;161:68–73.
[29] Liu P, Yin GP, Du CY. Composite anode catalyst layer for direct methanol fuel cell. Electrochemistry Communications 2008;10:1471–3.
[30] Hottinen T, Mikkola M, Mennola T, Lund P. Titanium sinter as gas diffusion backing in PEMFC. Journal of Power Sources 2003;118:183–8.
[31] Dicks AL. Review: the role of carbon in fuel cells. Journal of Power Sources 2006;156:128–41.
[32] Cao J, Chen M, Chen J, Wang S, Zou Z, Li Z, et al. Double microporous layer cathode for membrane electrode assembly of passive direct methanol fuel cells. International Journal of Hydrogen Energy 2010;35:4622–9.
[33] Yury G. Nanomaterials handbook. CRC Press LLC; 2006.
[34] Antolini E. Carbon supports for low-temperature fuel cell catalysts. Applied Catalysis B: Environmental 2009;88:1–24.
[35] Yuan T, Zou Z, Chen M, Li Z, Xia B, Yang H. New anodic diffusive layer for passive micro-direct methanol fuel cell. Journal of Power Sources 2009;192:423L 428.
[36] Wu QX, Zhao TS, Chen R, Yang WW. Effects of anode microporous layers made of carbon powder and nanotubes on water transport in direct methanol fuel cells. Journal of power sources 2009;191:304–11.
[37] Okada M, Konta Y, Nakagawa N. Carbon nano-fiber interlayer that provides high catalyst utilization in direct methanol fuel cell. Journal of Power Sources 2008;185:711–6.
[38] Wang T, Lin C, Fang Y, Ye F, Miao R, Wang X. A study on the dissymmetrical microporous layer structure of a direct methanol fuel cell. Electrochimica Acta 2008;54:781–5.
[39] Song KY, Lee HK, Kim HT. MEA design for low water crossover in air-breathing DMFC. Electrochimica Acta 2007;53:637–43.
[40] Tseng C-J, Lo S-K. Effects of microstructure characteristics of gas diffusion layer and microporous layer on the performance of PEMFC. Energy Conversion and Management 2010;51:677–84.
[41] Jeong SU, Cho EA, Kim HJ, Lim TH, Oh IH, Kim SH. A study on cathode structure and water transport in air-breathing PEM fuel cells. Journal of Power Sources 2006;159:1089–94.
[42] Zhang J, Yin GP, Lai QZ, Wang ZB, Cai KD, Liu P. The influence of anode gas diffusion layer on the performance of low-temperature DMFC. Journal of Power Sources 2007;168:453–8.
[43] Santiago EI, Ticianelli EA. The performance of carbon-supported PtOs electrocatalysts for the hydrogen oxidation in the presence of CO. International Journal of Hydrogen Energy 2005;30:159L 165.
[44] Grgur BN, Markovic NM, Ross PN. Electrooxidation of H_2, CO and H_2/CO mixtures on a well-characterized Pt ± Re bulk alloy electrode and comparison with other Pt binary alloys. *PII* 1998; S0013–4686:00120-0.
[45] Kim J, Momma T, Osaka T. Cell performance of Pd–Sn catalyst in passive direct methanol alkaline fuel cell using anion exchange membrane. Journal of Power Sources 2009;189:999–1002.
[46] Zhou X-W, Zhang R-H, Zhou Z-Y, Sun S-G. Preparation of PtNi hollow nanospheres for the electrocatalytic oxidation of methanol. Journal of Power Sources 2011;196:5844–8.
[47] Shen SY, Zhao TS, Xu JB. Carbon supported PtRh catalysts for ethanol oxidation in alkaline direct ethanol fuel cell. International Journal of Hydrogen Energy 2010;35:12911–7.
[48] Guo D-J. Electrooxidation of ethanol on novel multi-walled carbon nanotube supported platinum–antimony tin oxide nanoparticle catalysts. Journal of Power Sources 2011;196:679–82.
[49] Gurau B, Viswanathan R, Liu R, Lafrenz TJ, Ley KL, Smotkin ES. Structural and electrochemical characterization of binary, ternary, and quaternary platinum alloy catalysts for methanol electro-oxidation. Journal of Physical Chemistry B 1998;102:9997–10003.
[50] Ishihara A, Ohgi Y, Matsuzawa K, Mitsushima S, Ota K. Progress in nonprecious metal oxide-based cathode for polymer electrolyte fuel cells. Electrochimica Acta 2010;55:8005–12.
[51] Baglio V, Stassi A, Di Blasi A, D'Urso C, Antonucci V, Aricò AS. Investigation of bimetallic Pt–M/C as DMFC cathode catalysts. Electrochimica Acta 2007;53:1360–4.
[52] You DY, Kwon K, Pak C, Chang H. Platinum–antimony tin oxide nanoparticle as cathode catalyst for direct methanol fuel cell. Catalyst Today 2009;146:15–9.
[53] Zhai Y, Zhang H, Xing D, Shao Z-G. The stability of Pt/C catalyst in H_3PO_4/PBI PEMFC during high temperature life test. Journal of Power Sources 2007;164:126–33.
[54] Thiam HS, Daud WRW, Kamarudin SK, Mohammad AB, Kadhum AAH, Loh KS, Majlan EH. Overview on nano-structured membrane in fuel cell applications. International Journal of Hydrogen Energy 2011;35(4):3187–225.
[55] Rao V, Simonov PA, Savinova ER, Plaksin GV, Cherepanova SV, Kryukova GN, et al. The influence of carbon support porosity on the activity of PtRu/Sibunit anode catalysts for methanol oxidation. Journal of Power Sources 2005;145:178–87.
[56] Zainoodin AM, Kamarudin SK, Daud WRW. Electrode in direct methanol fuel cells. International Journal of Hydrogen Energy 2010;35(10):4606–21.
[57] Park CH, Scibioh MA, Kim H-J, Oh I-H, Hong S-A, Ha HY. Modification of carbon support to enhance performance of direct methanol fuel cell. Journal of Power Sources 2006;162:1023–8.
[58] Guo J, Sun G, Wang Q, Wang G, Zhou Z, Tang S, et al. Carbon nanofibers supported Pt–Ru electrocatalysts for direct methanol fuel cells. Carbon 2006;44:152–7.
[59] Wu G, Xu B-Q. Carbon nanotube supported Pt electrodes for methanol oxidation: a comparison between multi- and single-walled carbon nanotubes. Journal of Power Sources 2007;174:148–58.
[60] Jha N, Reddy ALM, Shaijumon MM, Rajalakshmi N, Ramaprabhu S. Pt–Ru/multi-walled carbon nanotubes as electrocatalysts for direct methanol fuel cell. International Journal of Hydrogen Energy 2008;33:427–33.
[61] Chen Y, Zhang G, Ma J, Zhou Y, Tang Y, Lu T. Electro-oxidation of methanol at the different carbon materials supported Pt nano-particles. International Journal of Hydrogen Energy 2010;35:10109–17.
[62] Chiang Y-C, Ciou J-R. Effects of surface chemical states of carbon nanotubes supported Pt nanoparticles on performance of proton exchange membrane fuel cells. International Journal of Hydrogen Energy 2011;36:6826–31.
[63] Antolini E. Composite materials: an emerging class of fuel cell catalyst supports. Applied Catalysis B: Environmental 2010;100:413–26.
[64] Zheng J-S, Zhang X-S, Li P, Zhou X-G, Yuan W-K. Microstructure effect of carbon nanofiber on electrocatalytic oxygen reduction reaction. Catalysis Today 2008;131:270–7.
[65] Bessel CA, Laubernds K, Rodriguez NM, Baker RTK. Graphite nanofibers as an electrode for fuel cell applications. Journal of Physical Chemistry B 2001;105:1115–8.
[66] Ismagilov ZR, Kerzhentsev MA, Shikina NV, Lisitsyn AS, Okhlopkova LB, Barnakov ChN, Sakashita M, Iijima T, Tadokoro K. Development of active catalysts for low Pt loading cathodes of PEMFC by surface tailoring of nanocarbon materials. Catalysis Today 2005;102–3:58–66.
[67] Park K-W, Sung Y-E. Origin of the enhanced catalytic activity of carbon nanocoil-supported PtRu alloy electrocatalysts. Journal of Physical Chemistry B 2004;108:939–44.
[68] Lebert M, Kaempgen M, Soehn M, Wirth T, Roth S, Nicoloso N. Fuel cell electrodes using carbon nanostructures. Catalysis Today 2009;143:64–8.
[69] Liu H, Song C, Zhang L, Zhang J, Wang H, Wilkinson DP. A review of anode catalysis in the direct methanol fuel cell. Journal of Power Sources 2006;155:95–110.
[70] Tang Z, Poh CK, Tian Z, Lin J, Ng HY, Chua DHC. In situ grown carbon nanotubes on carbon paper as integrated gas diffusion and catalyst layer for proton exchange membrane fuel cells. Electrochimica Acta 2011;56:4327–34.
[71] Bae B, Kho BK, Lim TH, Oh IH, Hong SA, Ha HY. Performance evaluation of passive DMFC single cells. Journal of Power Sources 2006;158:1256–61.
[72] Ahmad MM, Kamarudin SK, Daud WRW, Yaakub Z. High power passive μDMFC with low catalyst loading for small power generation. Energy Conversion and Management 2010;51:821–5.
[73] Zhao X, Fan X, Wang S, Yang S, Yi B, Xin Q, et al. Determination of ionic resistance and optimal composition in the anodic catalyst layers of DMFC using AC impedance. Journal of Hydrogen Energy 2005;30:1003–10.
[74] Shimizu T, Momma T, Mohamedi M, Osaka T, Sarangapani S. Design and fabrication of pumpless small direct methanol fuel cells for portable applications. Journal of Power Sources 2004;137:277–83.

[75] Abdelkareem MA, Tsujiguchi T, Nakagawa N. Effect of black catalyst ionomer content on the performance of passive DMFC. Journal of Power Sources 2010;195:6287–93.
[76] Morgan RD, Haan JL, Masel RI. Effects of Nafion loading in anode catalyst inks on the miniature direct formic acid fuel cell. Journal of Power Sources 2010;195:6405–10.
[77] Kim KH, Lee K-Y, Kim H-J, Cho EA, Lee S-Y, Lim T-H, et al. The effects of Nafion ionomer content in PEMFC MEAs prepared by a catalyst-coated membrane (CCM) spraying method. International Journal of Hydrogen Energy 2010;35:2119–26.
[78] Jeng K-T, Chien C-C, Hsu N-Y, Huang W-M, Chiou S-D, Lin S-H. Fabrication and impedance studies of DMFC anode incorporated with CNT-supported high-metal-content electrocatalyst. Journal of Power Sources 2007;164:33–41.
[79] Dohle H, Schmitz H, Bewer T, Mergel J, Stolten D. Development of a compact 500 W class direct methanol fuel cell stack. Journal of Power Sources 2002;106:313–22.
[80] Umeda J, Suzuki M, Kato M, Moriya M, Sakamoto W, Yogo T. Proton conductive inorganic–organic hybrid membranes functionalized with phosphonic acid for polymer electrolyte fuel cell. Journal of Power Sources 2010;195:5882–8.
[81] Chu Y-H, Shul YG, Choi WC, Woo SI, Han H-S. Evaluation of the Nafion effect on the activity of Pt–Ru electrocatalysts for the electro-oxidation of methanol. Journal of Power Sources 2003;118:334–41.
[82] Bunazawa H, Yamazaki Y. Influence of anion ionomer content and silver cathode catalyst on the performance of alkaline membrane electrode assemblies (MEAs) for direct methanol fuel cells (DMFCs). Journal of Power Sources 2008;182:48–51.
[83] Lee JK, Li W, Manthiram A. Sulfonated poly(ether ether ketone) as an ionomer for direct methanol fuel cell electrodes. Journal of Power Sources 2008;180:56–62.
[84] Choi HJ, Kim J, Kwon Y, Han J. Comparative study of three different catalyst coating methods for direct methanol fuel cells. Journal of Power Sources 2010;195:160–4.
[85] Yang T. Preliminary study of SPEEK/PVA blend membranes for DMFC applications. Journal of Hydrogen Energy 2008;33:6772–9.
[86] Kim HJ, Kim HJ, Shul YG, Han HS. Nafion–Nafion/polyvinylidene fluoride–Nafion laminated polymer membrane for direct methanol fuel cells. Journal of Power Sources 2004;135:66–71.
[87] Ma ZQ, Cheng P, Zhao TS. A palladium-alloy deposited Nafion membrane for direct methanol fuel cells. Journal of Membrane Science 2003;215: 327–36.
[88] Park J-S, Krishnan P, Park S-H, Park G-G, Yang T-H, Lee W-Y, et al. A study on fabrication of sulfonated poly(ether ether ketone)-based membrane electrode assemblies for polymer electrolyte membrane fuel cell. Journal of Power Sources 2008;178:642–50.
[89] Mikhailenko SD, Zaidi SMJ, Kaliaguine S. Sulfonated polyether ether ketone based composite polymer electrolyte membranes. Catalysis Today 2001;67:225–36.
[90] Smitha B, Sridhar S, Khan AA. Synthesis and characterization of proton conducting polymer membranes for fuel cells. Journal of Membrane Science 2003;225:63–76.
[91] Karlsson LE, Jannasch P. Polysulfone ionomers for proton conducting fuel cell membranes: sulfoalkylated polysulfones. Journal of Membrane Science 2004;230:61–70.
[92] Ainla A, Brandell D. Nafion–polybenzimidazole (PBI) composite membranes for DMFC applications. Solid State Ionics 2007;178:581–5.
[93] Xing P, Robertson GP, Guiver MD, Mikhailenko SD, Wang K, Kaliaguine S. Synthesis and characterization of sulfonated poly(ether ether ketone) for proton exchange membranes. Journal of Membrane Science 2004;229:95–106.
[94] Ren S, Sun G, Li C, Liang Z, Wu Z, Jin W, et al. Organic silica/Nafion® composite membrane for direct methanol fuel cells. Journal of Membrane Science 2006;282:450–5.
[95] Kim HK, Chang H. Organic/inorganic hybrid membranes for direct methanol fuel cells. Journal of Membrane Science 2007;288:188–94.
[96] Charinpanitkul T, Faungnawakij K, Tanthapanichakoon W. Review of recent research on nanoparticle production in Thailand. Advanced Powder Technology 2008;19(5):443–57.
[97] Liang ZX, Zhao TS, Prabhuram J. A glue method for fabricating membrane electrode assemblies for direct methanol fuel cells. Electrochimica Acta 2006;51:6412–8.
[98] Wang S, Sun G, Wang G, Zhou Z, Zhao X, Sun H, et al. Improvement of direct methanol fuel cell performance by modifying catalyst coated membrane structure. Electrochemistry Communications 2005;7:1007–12.
[99] Wang T, Lin C, Ye F, Fang Y, Li J, Wang X. MEA with double-layered catalyst cathode to mitigate methanol crossover in DMFC. Electrochemistry Communications 2008;10:1261–3.
[100] Prasanna M, Cho EA, Lim T-H, Oh IH. Effects of MEA fabrication method on durability of polymer electrolyte membrane fuel cells. Electrochimica Acta 2008;53:5434–41.
[101] Qiao J, Li B, Yang D, Ma J. High PEMFC performance by applying Ir–V nanoparticles as a cathode catalyst. Applied Catalysis B: Environmental 2009;91:198–203.
[102] Krishnan NN, Prabhuram J, Hong YT, Kim H-J, Yoon K, Ha H-Y, et al. Fabrication of MEA with hydrocarbon based membranes using low temperature decal method for DMFC. International Journal of Hydrogen Energy 2010;35:5647–55.
[103] Tang H, Wang S, Pan M, Jiang SP, Ruan Y. Performance of direct methanol fuel cells prepared by hot-pressed MEA and catalyst-coated membrane (CCM). Electrochimica Acta 2007;52:3714–8.